J. metamorphic Geol., 2010, **28,** 317–339 doi:10.1111/j.1525-1314.2010.00865.x

Metamorphic history of eclogites and country rock gneisses in the Aktyuz area, Northern Tien-Shan, Kyrgyzstan: a record from initiation of subduction through to oceanic closure by continent–continent collision

R. T. OROZBAEV,[1,2] A. TAKASU,[1] A. B. BAKIROV,[2] M. TAGIRI[3] AND K. S. SAKIEV[2]
[1]*Department of Geoscience, Shimane University, 1060 Nishikawatsu, Matsue, Shimane 690-8504, Japan (r.t.orozbaev@gmail.com)*
[2]*Institute of Geology, Kyrgyz National Academy of Science, 30 Erkindik Avenue, Bishkek 720481, Kyrgyzstan*
[3]*Office of Institutional Research, Ibaraki University, 2-1-1, Bunkyo, Mito 310-8512, Japan*

ABSTRACT Eclogites and related high-*P* metamorphic rocks occur in the Zaili Range of the Northern Kyrgyz Tien-Shan (Tianshan) Mountains, which are located in the south-western segment of the Central Asian Orogenic Belt. Eclogites are preserved in the cores of garnet amphibolites and amphibolites that occur in the Aktyuz area as boudins and layers (up to 2000 m in length) within country rock gneisses. The textures and mineral chemistry of the Aktyuz eclogites, garnet amphibolites and country rock gneisses record three distinct metamorphic events (M1–M3). In the eclogites, the first MP–HT metamorphic event (M1) of amphibolite/epidote-amphibolite facies conditions (560–650 °C, 4–10 kbar) is established from relict mineral assemblages of polyphase inclusions in the cores and mantles of garnet, i.e. Mg-taramite + Fe-staurolite + paragonite ± oligoclase ($An_{<16}$) ± hematite. The eclogites also record the second HP-LT metamorphism (M2) with a prograde stage passing through epidote-blueschist facies conditions (330–570 °C, 8–16 kbar) to peak metamorphism in the eclogite facies (550–660 °C, 21–23 kbar) and subsequent retrograde metamorphism to epidote-amphibolite facies conditions (545–565 °C and 10–11 kbar) that defines a clockwise *P–T* path. THERMOCALC (average *P–T* mode) calculations and other geothermobarometers have been applied for the estimation of *P–T* conditions. M3 is inferred from the garnet amphibolites and country rock gneisses. Garnet amphibolites that underwent this pervasive HP–HT metamorphism after the eclogite facies equilibrium have a peak metamorphic assemblage of garnet and pargasite. The prograde and peak metamorphic conditions of the garnet amphibolites are estimated to be 600–640 °C; 11–12 kbar and 675–735 °C and 14–15 kbar, respectively. Inclusion phases in porphyroblastic plagioclase in the country rock gneisses suggest a prograde stage of the epidote-amphibolite facies (477 °C and 10 kbar). The peak mineral assemblage of the country rock gneisses of garnet, plagioclase ($An_{11–16}$), phengite, biotite, quartz and rutile indicate 635–745 °C and 13–15 kbar. The *P–T* conditions estimated for the prograde, peak and retrograde stages in garnet amphibolite and country rock are similar, implying that the third metamorphic event in the garnet amphibolites was correlated with the metamorphism in the country rock gneisses. The eclogites also show evidence of the third metamorphic event with development of the prograde mineral assemblage pargasite, oligoclase and biotite after the retrograde epidote-amphibolite facies metamorphism. The three metamorphic events occurred in distinct tectonic settings: (i) metamorphism along the hot hangingwall at the inception of subduction, (ii) subsequent subduction zone metamorphism of the oceanic plate and exhumation, and (iii) continent–continent collision and exhumation of the entire metamorphic sequences. These tectonic processes document the initial stage of closure of a palaeo-ocean subduction to its completion by continent–continent collision.

Key words: Aktyuz; country rock gneiss; eclogite; Kyrgyz Tien-Shan; polyphase metamorphism.

INTRODUCTION

Eclogites frequently occur as blocks in country rocks, as described from the Western Gneiss Region (Smith, 1988; Engvik & Andersen, 2000), the Dora-Maira Massif (Chopin, 1984; Compagnoni *et al.*, 1995), the Bohemian Massif (Medaris *et al.*, 1998; Štípská *et al.*, 2006), the Kokchetav Massif (Dobretsov *et al.*, 1995; Katayama *et al.*, 2000), the Sambagawa belt (Takasu, 1984; Aoya, 2001), the Franciscan Complex (Ernst, 1971; Moore, 1984), the North Qaidam-Altun belt (Song *et al.*, 2003; Yang *et al.*, 2005) and the Dabie–Sulu terrane (Wang *et al.*, 1989; Enami & Nagasaki, 1999; Liu *et al.*, 2009). High-pressure (HP) and

ultrahigh-pressure (UHP) mafic rocks and their country rocks generally have complex pressure–temperature (*P–T*) histories. The presence of coesite and/or diamond in both eclogites and surrounding gneisses in the Dora-Maira Massif, Kokchetav Massif, the North Qaidam and the Dabie-Sulu terranes demonstrates that in these cases both rock types were carried to great depths (more than 100 km), experiencing UHP metamorphism together, and sharing their entire *P–T* history. In contrast, tectonic blocks of HP mafic rocks within metapelites are considered to result from tectonic mixing, with juxtaposition at relatively lower pressure. Examples are found in the Sambagawa belt of Japan (Takasu, 1984, 1989; Miyagi & Takasu, 2005), the Franciscan Complex (Moore, 1984), the Alanya nappes in Turkey (Okay, 1989), and the Bohemian Massif in Eastern Europe (Štípská *et al*., 2006). In these cases, the country rocks did not share the prograde and peak *P–T* conditions of the eclogites, but underwent only relatively low-*P*/T metamorphism after their juxtaposition.

An alternative *P–T* path for HP mafic rocks and country rock gneisses has been proposed. This has a complex, so-called β-shape metamorphic *P–T* path, as seen in the Internal Penninic Nappes in the Western Alps (Kurz & Froitzheim, 2002) and in the Snowbird tectonic zone in the Canadian Shield (Baldwin *et al*., 2007). The authors considered that *P–T* paths of this type were created by two superimposed metamorphic events, and that the latest event was accomplished mainly by high-temperature and medium-pressure amphibolite facies overprint, i.e. heating and simultaneous decrease in pressure.

In this study, we report a β-shape metamorphic *P–T* path from eclogites and garnet amphibolites exposed in the Aktyuz area in the Zaili Range of Kyrgyz Tien-Shan Mountains (Fig. 1), where the latest metamorphic event records relatively HP metamorphism. Tagiri *et al*. (1995) estimated that the peak metamorphic conditions of the Aktyuz eclogites were 600 °C and >12 kbar. Orozbaev *et al*. (2007) proposed two metamorphic events for the Aktyuz eclogites, i.e. a pre-eclogitic, relatively medium-pressure and high-temperature (MP-HT) metamorphic event of amphibolite facies conditions (560–650 °C, 4–10 kbar) and high-pressure and low-temperature (HP-LT) eclogitic metamorphic event with the prograde epidote-blueschist facies (330–570 °C, 8–16 kbar) and peak eclogite facies (600–710 °C, 15–25 kbar) conditions.

New petrological and geothermobarometric evidence for the peak conditions of the Aktyuz eclogites and subsequent metamorphic history are obtained. The *P–T* paths and metamorphic evolution of the garnet amphibolites located at the margin of the eclogite body, along with surrounding country rock gneisses are discussed. We further suggest the occurrence of a third high-pressure and high-temperature (HP–HT) metamorphic event after the second HP-LT eclogitic metamorphic event. The *P–T* evolution of the Aktyuz HP metamorphic rocks depicted by this study reconstructs the entire tectonic sequence from inception of oceanic plate subduction to continent–continent collision, and thus is a typical example of the history of a palaeo-ocean closure in the Central Asian Orogenic Belt (CAOB). This history includes the initial stage of subduction of oceanic crust beneath the continental crust with development of MP–HT metamorphism, documenting inception of palaeo-ocean closure; subsequent HP–LT metamorphism and exhumation within the subduction zone; and the completion of palaeo-ocean closure by continent–continent collision, with accompanying HP–HT metamorphism and exhumation of the entire metamorphic sequence.

GEOLOGICAL SETTING

Regional geology

The Tien-Shan (Tianshan) Mountains are located in the CAOB, and extend for ~2500 km from Tajikistan, through Kyrgyzstan, to north-west China (Şengör *et al*., 1993; Windley *et al*., 2007). Several HP–UHP metamorphic belts have been described in the Tien-Shan Mountains (Fig. 1a). The Fan-Karategin HP-LT metamorphic belt in South Tien-Shan of Tajikistan is regarded as an ancient subduction–accretionary complex (Volkova & Budanov, 1999). In the Chinese South Tien-Shan, eclogites and blueschists have been described from the western Tianshan HP–LT metamorphic belt (Gao *et al*., 1999; Klemd *et al*., 2002; Gao & Klemd, 2003; Wei *et al*., 2003; Lin & Enami, 2006; Zhang *et al*., 2007), and some of these eclogites record UHP metamorphic conditions (Zhang *et al*., 2005; Lü *et al*., 2009). The South Central Tien-Shan suture zone is regarded as a Late Devonian–Early Carboniferous (346–332 Ma: Gao & Klemd, 2003) and/or Permian–Triassic (233–226 Ma: Zhang *et al*., 2007) collisional zone.

The Kyrgyz Tien-Shan Mountains extend from east to west, separating the Kazakhstan plate to the north and the Tarim plate to the south. They are divided into three tectonic units; the Northern Tien-Shan, the Central (or Middle) Tien-Shan and the Southern Tien-Shan (Fig. 1a), bounded by major tectonic discontinuities including the Main Tectonic Line and the Atbashy-Inylchek, Talas-Fergana and South Fergana faults (e.g. Nikolaev, 1933; Burtman *et al*., 1996; Bakirov & Maksumova, 2001; Bakirov *et al*., 2003). HP–UHP metamorphic rocks occur at three localities in the Kyrgyz Tien-Shan. The Makbal and Aktyuz eclogite-bearing complexes occur within the Northern Tien-Shan, and the Atbashy complex is located in the Southern Tien-Shan (Fig. 1a) (Bakirov *et al*., 1974, 1998; Sobolev *et al*., 1986; Tagiri *et al*., 1995). Eclogites in the Makbal complex experienced HP metamorphism with variable *P–T* conditions (Tagiri *et al*., 1995; Bakirov *et al*., 2006), whereas coesite inclusions within garnet in garnet-chloritoid-talc schists and

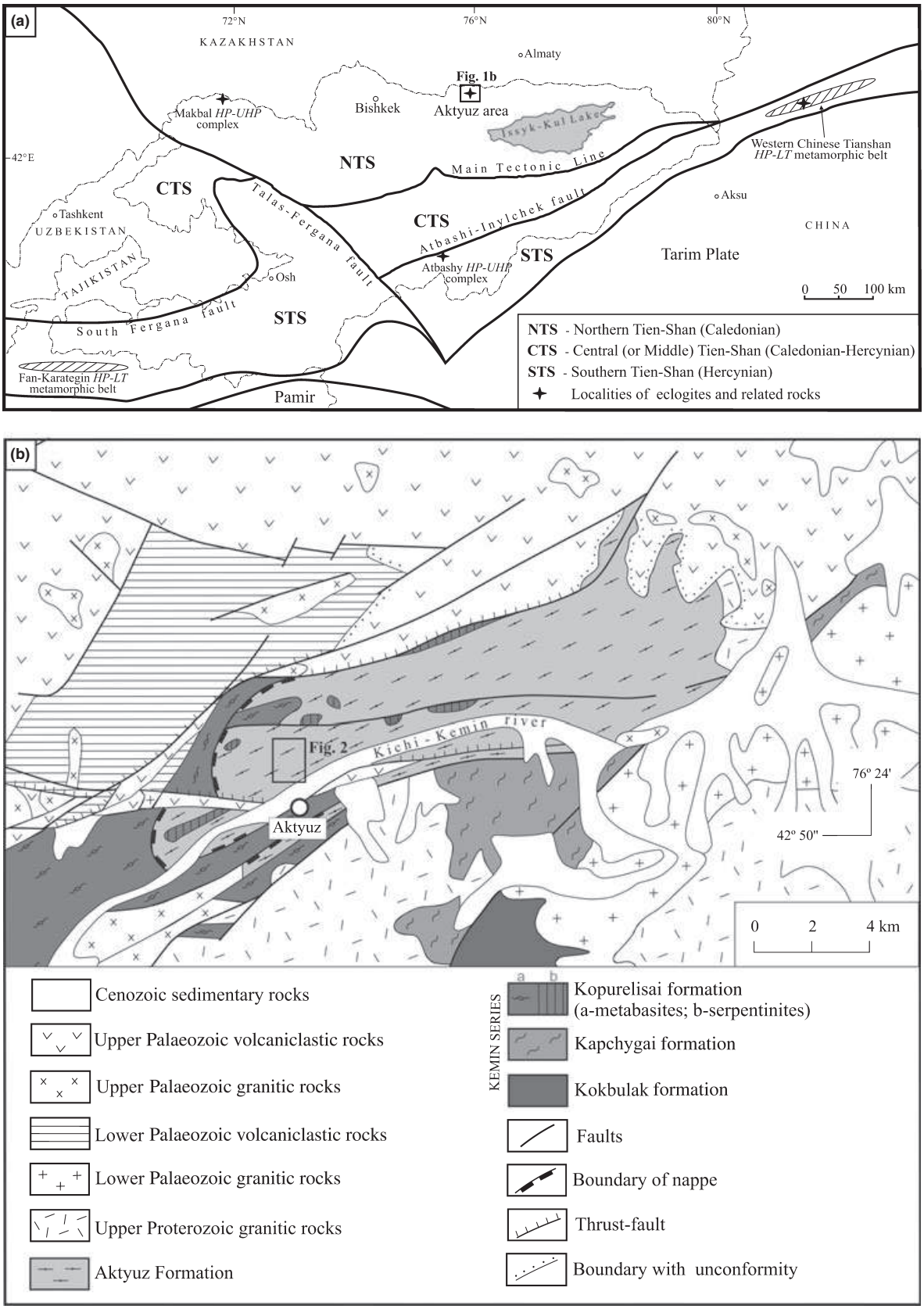

Fig. 1. (a) Simplified tectonic map of the Tien-Shan Mountains. (b) Geological map of the Aktyuz area (after Bakirov *et al.*, 2003).

quartzites suggest UHP conditions (> 25 kbar; < 600 °C) for the host rocks in the Makbal complex (Tagiri & Bakirov, 1990; Bakirov *et al.*, 1998; Ishida *et al.*, 2004; Tagiri *et al.*, 2006; Bakirov *et al.*, 2006). The peak UHP metamorphism in the Makbal complex is dated at 481 ± 26 Ma (Togonbaeva *et al.*, 2009).

Geology of the Aktyuz area

The other occurrence of eclogites in Northern Kyrgyz Tien-Shan lies in the Aktyuz area (Bakirov, 1989; Tagiri *et al.*, 1995; Bakirov *et al.*, 2003; Orozbaev *et al.*, 2007). It crops out in the Zaili Range of the Northern Tien-Shan, and includes the Aktyuz Formation and the Kemin Series (Fig. 1b) (Bakirov, 1978; Bakirov *et al.*, 2003). The Aktyuz Formation consists mainly of pelitic and granitic gneisses containing lenses and layers of eclogite, garnet amphibolite and amphibolite bodies (Fig. 2). The Kemin Series includes the Kopurelisai, Kapchygai and Kokbulak Formations (Fig. 1b). The Kopurelisai Formation consists of metagabbros, metabasalts, serpentinites and metapelites, and these are probably constituents of an ophiolite (Bakirov *et al.*, 2003). The Kapchygai Formation is composed of basic migmatites, amphibolites, metagabbros, eclogites, serpentinites and talc schists. The Kokbulak Formation consists of pelitic and carbonaceous migmatites, pelitic gneisses, siliceous schists and marbles. The Kemin Series is intruded by granitic rocks ranging from Upper Proterozoic to Upper Palaeozoic in age (Kiselev, 1999; Bakirov *et al.*, 2003; Djenchuraeva *et al.*, 2008).

Exposures of the Aktyuz Formation extend in E–W to NE–SW directions over a length of more than 20 km, with a width up to 5 km. The Aktyuz Formation is covered by Upper Palaeozoic volcaniclastic rocks in the north and northeast (Fig. 1b) (Bakirov, 1978; Bakirov *et al.*, 2003). According to Bakirov *et al.* (2003), the Aktyuz Formation is an allochthonous nappe that was thrust over on the Kopurelisai Formation.

The Aktyuz Formation consists of various types of gneisses containing intercalated layers and lenses of eclogites, garnet amphibolites and amphibolites varying from 0.5 to 70 m in thickness and from 3 to 2000 m in length (Fig. 2). The country rock gneisses consist of alternating grey pelitic gneiss and red granitic gneiss. The thickness of the interbedding of these gneisses varies from a few centimetres to several metres, producing rocks with migmatitic texture, and suggesting a partial melting within the country rock gneisses. Several granite-porphyry dykes intrude the Aktyuz Formation. Eclogites are preserved in the central parts of the garnet amphibolite bodies (Fig. 2). The eclogites are massive, whereas the garnet amphibolites and amphibolites in the margins of the bodies show a weak foliation parallel to that of the surrounding gneisses. Well preserved eclogites occur in the south-western part of this area. This eclogite body is lenticular in form, and has a width of ~60 m and length of 500 m (Fig. 2).

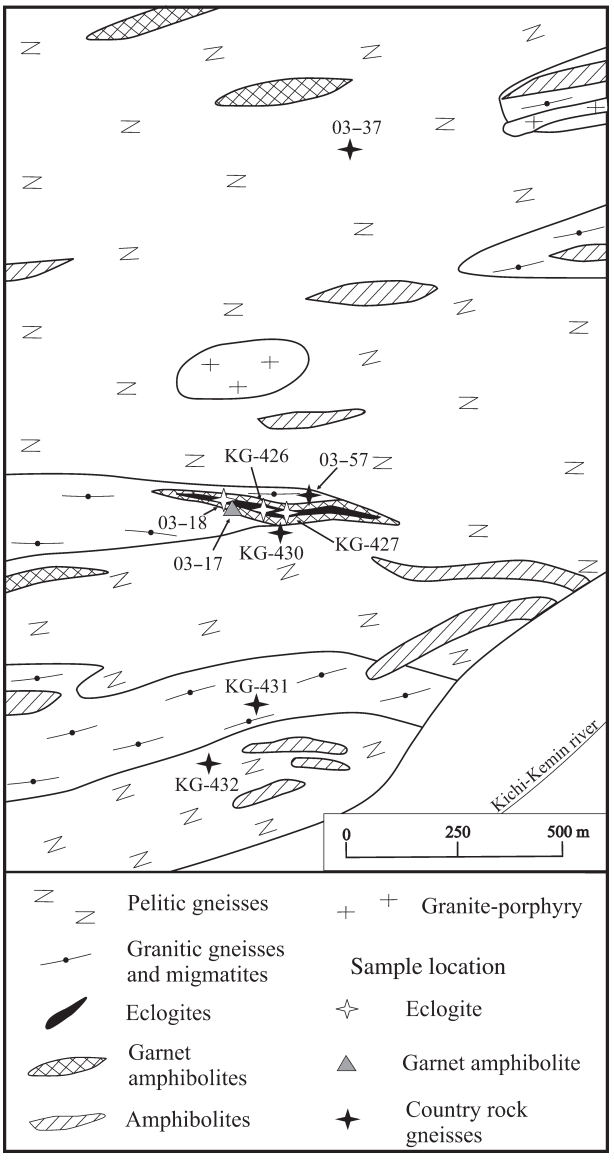

Fig. 2. Geological map of the Aktyuz Formation and sample locations.

Bakirov & Korolev (1979) reported U–Pb zircon ages of 2780 ± 300 and 1820 ± 180 Ma for Aktyuz Formation gneisses and ages of 2550 ± 250 to 1960 ± 200 Ma from migmatites of the Kemin Series. Kiselev *et al.* (1993) reported U–Pb zircon ages of 1720 ± 20 and 560 ± 11 Ma for pelitic gneisses and migmatites of the Kemin Series, respectively. The above ages were obtained from zircon concentrates, and thus the wide range of ages probably represents the ages of both detrital and metamorphic zircon. A Rb–Sr mineral isochron age of 749 ± 14 Ma was reported by Tagiri *et al.* (1995), and this was regarded as the peak metamorphic age of the Aktyuz eclogite.

The granite intrusion in the southwest of the Aktyuz Formation has a SHRIMP zircon age of 416 Ma (Konopelko *et al*., 2006), suggesting that metamorphism of the country rock gneisses was completed before that time.

PETROGRAPHY

The mineral abbreviations used in the text, tables and figures follow Whitney & Evans (2010) except for Olg = oligoclase.

Eclogites

Samples of eclogites (KG-426, KG-427 & 03–18) described in this study were collected from the inner part of the eclogite-garnet amphibolite body (Fig. 2). The eclogites are medium- to coarse-grained, and have granoblastic texture (Fig. 3a). They consist mainly of garnet, clinopyroxene, Na–Ca- & Ca-amphibole and phengite, with minor plagioclase, epidote, paragonite, quartz, K-feldspar, Na-amphibole (glaucophane), biotite, chlorite, rutile, ilmenite, titanite and hematite. Accessory amounts of apatite, staurolite and zircon occasionally occur.

Garnet occurs as inclusions in clinopyroxene (Fig. 3a) and as discrete grains in the matrix (Fig. 3-a,b,d,e). Garnet grains are subhedral to anhedral, up to 2 mm in diameter, with zoning from pale red cores to colourless rims. Garnet contains inclusions of Na–Ca-amphibole and rare Na-amphibole (glaucophane), clinopyroxene, paragonite, phengite, epidote, albite, rutile, hematite, and quartz (Fig. 3a,d,e). Polyphase inclusions with assemblages of Mg-taramite + Fe-staurolite + paragonite ± hematite, Mg-taramite + Fe-staurolite + oligoclase ($An_{<16}$), paragonite + Fe-staurolite + oligoclase ($An_{<16}$) and/or paragonite + Fe-staurolite also occur in the core and the mantle of garnet (Orozbaev *et al*., 2007). Garnet is partly replaced by aggregates consisting of Na–Ca-amphibole and plagioclase ($An_{5–13}$) (Fig. 3a,b) or by Na–Ca- and Ca-amphiboles, chlorite and biotite along the rim and cracks.

Clinopyroxene has three modes of occurrence. The first (Cpx1) occurs as inclusions in garnet (e.g. Fig. 3a,d), the second (Cpx2) occurs in the matrix, and the third (Cpx3) is a constituent of symplectites with plagioclase ($An_{2–9}$) after Cpx2 (Fig. 3b,c). Cpx2 forms subhedral prismatic crystals up to 10 mm (Fig. 3a,b,c) containing inclusions of Na-, Na–Ca- and Ca-amphiboles (e.g. glaucophane, barroisite, Mg-katophorite, winchite, actinolite and edenite), rutile, albite and quartz (Orozbaev *et al*., 2007). Cpx3 + Pl2 symplectite also occurs as inclusions in porphyroblastic amphibole (Amp3) in retrograded eclogites (e.g. sample 03–18; Fig. 3d).

Amphibole has three modes of occurrence. Amp1 forms inclusions in garnet, Cpx2 and Ph2, and has been already described by Orozbaev *et al*. (2007). Amp2 (Na–Ca & Ca-amphiboles) comprises discrete grains in the matrix, and also occurs at the contact between garnet and Cpx2 as a constituent of aggregates consisting of amphibole and plagioclase after garnet (Fig. 3a–c). Amp2 occurs as subhedral to anhedral prismatic crystals up to 0.5 mm long, and at the core has pleochroism of X' = bluish green to brownish green and Z' = green to deep green; rims have similar pleochroism but with slightly paler colour. Amp3 (Na–Ca and Ca-amphiboles) occurs as subhedral to euhedral porphyroblasts up to 3 mm across in severely amphibolitized eclogites (sample 03–18; Fig. 3d,e). It contains Cpx2, garnet, phengite, epidote, rutile and ilmenite as inclusions (Fig. 3d,e). This amphibole also contains aggregates of Cpx3 + Pl2 (Fig. 3d) as inclusions. Amp3 occasionally occurs as small euhedral prismatic grains near plagioclase and biotite symplectites (Fig. 3f). Amp3 is sometimes replaced by biotite or chlorite at its margins.

Phengite (Ph1) and paragonite (Pg1) inclusions in garnet have been described by Orozbaev *et al*. (2007). Ph2 grains reaching 1.5 mm across coexist with garnet and Cpx2 in the matrix of eclogites (Fig. 3a). The rim of Ph2 grains are replaced by a symplectitic aggregate consisting of biotite and plagioclase ($An_{11–22}$) (Fig. 3f). Phengite (possibly Ph2) inclusions up to 0.4 mm across occur within Amp3 (Fig. 3d,e). Pg2 has a maximum size of 0.5 mm, and occasionally coexists with Ph2 in the matrix. Biotite is a constituent of biotite + plagioclase symplectite after Ph2 (Fig. 3f).

Plagioclase occurs in three modes. Pl1 ($An_{4–16}$) occurs as inclusions in garnet and Cpx2 (Orozbaev *et al*., 2007). Pl2 in the matrix is optically and chemically zoned, from $An_{3–9}$ in the core to $An_{10–21}$ in the rim (Fig. 3e). Also, Pl2 is a constituent of symplectites with Cpx3 or Amp2 (Fig. 3b,c). Pl3 is a constituent of symplectite with biotite after Ph2 (Fig. 3f).

Epidote occurs as inclusions in garnet (Ep1) and as subhedral to euhedral prismatic grains up to 0.5 mm across in the matrix (Ep2) (Fig. 3c). Ep2 is zoned with pale brownish Sr and REE-rich cores to colourless Sr and REE-poor rims. Ep2 occasionally occurs as inclusions in Ph2 (Fig. 3f) and Amp3 (Fig. 3d,e). Rutile occurs as inclusions in garnet and Cpx2, and rutile in the matrix is occasionally surrounded by titanite or ilmenite.

Garnet amphibolite

Garnet amphibolite occurs in the margins of the eclogite-garnet amphibolite body (sample 03–17; Fig. 2), and consist mainly of amphibole, garnet, plagioclase and chlorite with minor biotite, K-feldspar, quartz, ilmenite, titanite, rutile, calcite and apatite. A weak schistosity defined by preferred orientation of amphibole is developed at the margin of the body, with orientation parallel to that of the surrounding gneisses.

Garnet consists mostly of subhedral grains up to 0.5 mm across (Fig. 4b,c) occurring in the matrix, and

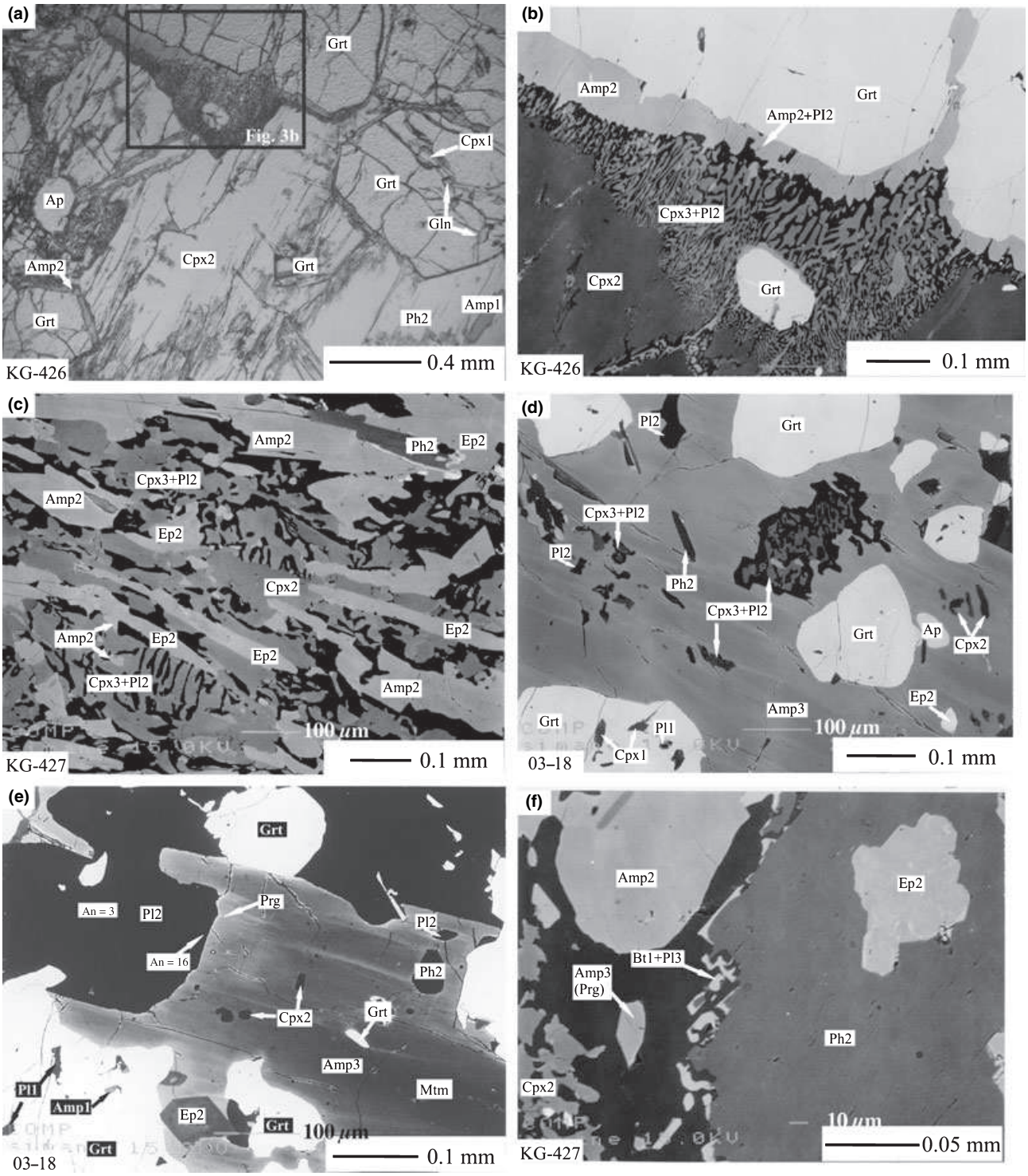

Fig. 3. Photomicrographs and backscattered electron images (BEI) showing textures in the eclogites. (a) Garnet is included within Cpx2. Garnet, Cpx2 and Ph2 coexist in the matrix. Amp1 is included within Ph2, whereas Amp2 is developed between garnet and Cpx2 (KG-426; open nicol); (b) Cpx3-Pl2 symplectites after Cpx2. Amp2 is developed at the boundary between garnet and Cpx2 (KG-426; BEI); (c) Retrograde mineral assemblages of Ep2, Amp2, Ph2 and symplectite of Cpx3 + Pl2 after Cpx2, define a weak schistosity (KG-427; BEI); (d) Porphyroblastic Amp3 containing garnet, Cpx2, Ph2, Ep2, Pl2 and symplectitic aggregate of Cpx3 + Pl2 as inclusions (03-18; BEI); (e) Amp3 containing inclusions of garnet, Cpx2, Ph2, Ep2 and Pl2, and showing zoning from Mg-taramite core to pargasite rim. The rim of Amp3 coexists with the rim of Pl2 (An_{16}). Garnet contains Amp1 and Pl1 inclusions (03-18; BEI); (f) Symplectite of Bt + Pl3 is developed after Ph2; euhedral prismatic Amp3 occurs nearby (KG-427; BEI).

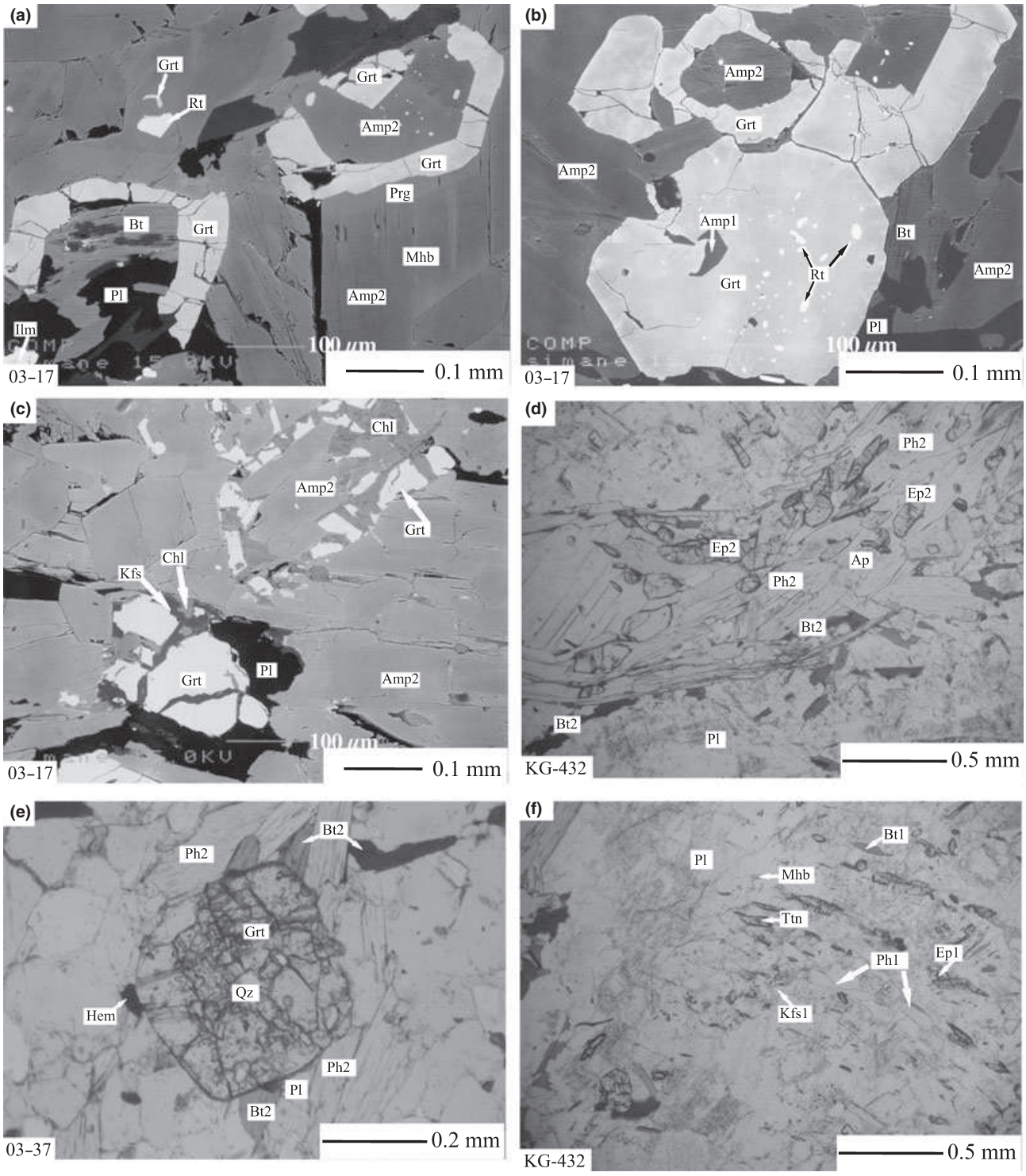

Fig. 4. Photomicrographs and BEI showing the textures in garnet amphibolites (a–c) and pelitic gneisses (d–f). (a) Amp2 in the matrix contains garnet and rutile inclusions and it is zoned from Mg-hornblende core to pargasite rim. Amp2 coexists with atoll garnet. Amp2 fills the interior of atoll garnet and is later replaced by biotite and plagioclase (03-17; BEI); (b) Garnet (with Amp1 and rutile in the mantle) and atoll garnet (with Amp2 in the core) coexisting with Amp2 in the matrix (03-17; BEI); (c) Garnet is replaced by chlorite, K-feldspar and plagioclase (03-17; BEI); (d) Plagioclase, Ep2, Ph2 and Bt2 in the matrix of the pelitic gneisses (KG-432; open nicol); (e) Garnet containing inclusions of quartz occurs with Ph2, plagioclase and Bt2 in the matrix (03-37; open nicol); (f) Porphyroblastic plagioclase containing Ph1, Ep1, Kfs1, Bt1, Mg-hornblende and titanite as inclusions (KG-432; open nicol).

containing inclusions of Ca-amphibole, rutile and quartz. Garnet occurs also as inclusions in Ca-amphibole (Fig. 4a) and as atoll garnet with interiors filled by Ca-amphibole (Fig. 4a-c). Garnet is partly replaced by chlorite, K-feldspar and biotite at the rim and along cracks (Fig. 4c).

Amphibole has two modes of occurrence. Amp1 (Ca-amphibole) is represented by subhedral prismatic crystals up to 0.1 mm across occurring as inclusions in garnet (Fig. 4b). Amp2 (Ca-amphibole) consists of subhedral prismatic crystals up to 1 mm within the matrix (Fig. 4a–c), and exhibits zoning with X′ = pale green and Z′ = pale brownish green cores to X′ = bluish-green and Z′ = green rims. It contains inclusions of garnet, rutile and ilmenite, and is replaced by chlorite and biotite along its rims. Amp2 (Ca-amphibole) occurs also in the interior of atoll garnet (Fig. 4a–c), and is replaced by any combination of chlorite, plagioclase, biotite and K-feldspar (Fig. 4a).

Plagioclase ($An_{12–18}$) and K-feldspar ($Or_{98–99}$) grains up to 0.5 mm across replace garnet and Amp2 (Fig. 4a–c). Biotite (up to 0.5 mm) replaces garnet and Amp2 (Fig. 4a,b). Rutile occurs as inclusions in garnet and Amp2 (Fig. 4a,b), and rutile in the matrix is partially or completely replaced by ilmenite or titanite.

Country rock gneisses

Pelitic gneisses

The pelitic gneisses (samples 03–37, KG-430 & KG-432) consist mainly of plagioclase, phengite, biotite and quartz with minor garnet, epidote, chlorite, K-feldspar, Ca-amphibole, apatite, calcite, rutile, titanite, ilmenite, hematite and zircon. Preferred orientation of phengite and biotite define a schistosity (Fig. 4d).

Garnet occurs as inclusions in plagioclase and phengite (sample 03–37), and as discrete grains in the matrix. Garnet occurs as subhedral to euhedral crystals up to 1.5 mm across (Fig. 4e), and exhibits zoning from pale red cores to colourless rims. Garnet contains inclusions of quartz, phengite, rutile, apatite and rare zircon, and is partly or entirely replaced by chlorite, biotite and epidote.

Plagioclase occurs as subhedral prismatic grains up to 4 mm across containing inclusions of quartz, epidote, phengite, K-feldspar, biotite, Ca-amphibole, apatite, titanite, rutile and ilmenite (Fig. 4f). Ca-amphibole (e.g. Mg-hornblende) occurs locally as inclusions in plagioclase.

Phengite (Ph1) inclusions occur within porphyroblastic plagioclase (Fig. 4f; samples 03–37 & KG-432), garnet (sample KG-430), and occasionally in zircon. Ph2 grains up to 2 mm across containing inclusions of epidote, garnet, quartz, rutile and zircon occur in the matrix (Fig. 4d,e). Ph2 is occasionally replaced by chlorite and biotite at its rim. Biotite occurs in two modes. Bt1 occurs as inclusions in porphyroblastic plagioclase (Fig. 4f). Bt2 forms discrete grains up to 1 mm in the matrix (Fig. 4d,e) and replaces garnet and Ph2.

Epidote occurs both as inclusions (Ep1) in plagioclase (Fig. 4f) and Ph2, and as discrete grains (Ep2) in the matrix (Fig. 4d). Rutile is surrounded by ilmenite or titanite. Zircon is found as subhedral to euhedral prismatic crystals up to 0.2 mm long, containing inclusions of quartz, apatite, Ph1, epidote, K-feldspar, biotite and chlorite.

Granitic gneisses

Granitic gneisses (samples 03-57 & KG-431) consist mainly of K-feldspar, plagioclase and quartz with minor biotite, garnet, chlorite, ilmenite, hematite and zircon. K-feldspar (up to 1 mm) and plagioclase (up to 1.5 mm) in the matrix contain rare inclusions of quartz and zircon. Garnet occurs as subhedral to anhedral grains up to 1 mm across, containing quartz and rare biotite inclusions. Garnet is replaced by biotite and chlorite. Zircon occurs as subhedral to euhedral prismatic grains up to 0.2 mm long, and it contains inclusions of quartz, apatite, phengite, K-feldspar, albite ($An_{<2}$), biotite, chlorite, rutile, titanite and ilmenite.

MINERAL CHEMISTRY

Analytical procedures

Mineral compositions were determined using an electron probe microanalyser (JEOL JXA-8800M) at the Department of Geoscience, Shimane University. The analytical conditions used for all minerals were a 15 kV accelerating voltage, 20 nA beam current and 5 μm beam diameter. Corrections were carried out using the procedures of Bence & Albee (1968). Minute mineral inclusions (< 5 μm) in zircon separated from the country rock gneisses were examined by Raman spectroscopy at the Department of Earth and Planetary Materials Science, Tohoku University. Ferric iron contents in garnet and clinopyroxene were estimated on the basis of charge balance [$Fe^{3+} = 8 - 2Si - 2Ti - Al$ (for garnet)]; [$Fe^{3+} = 4 - 2Si - 2Ti - Al + Na$ (for clinopyroxene)]. Jadeite, aegirine and augite contents (mol.%) in clinopyroxene were estimated as $Jd = Al^{VI} * 100$, $Aeg = Na - Jd$ or $Aeg = Fe^{3+}$, if $(Na - Jd) \geq Fe^{3+}$, and $Aug = 100 - (Jd + Aeg)$, respectively. Ferric iron contents in amphibole were estimated as total cations $13 = Si + Al + Ti + Cr + Mg + Fe + Mn$ [(for O = 23; 13eCNK method of Schumacher, in Leake *et al.* (1997)], except for amphibole from garnet amphibolite (sample 03–17).

Garnet

Garnet in the eclogites, garnet amphibolites and country rock gneisses has almandine-rich composition with variable spessartine components (Table 1;

Table 1. Representative compositions of garnet.

Rock type	Eclogites									Garnet amphibolite						Pelitic gneiss					Granitic gneiss	
Sample	KG-426					KG-427		03–18		03–17						KG-430		03–37			03–57	
Mode		core	rim	rim	o-rim	core	rim	core	rim		core	mantle	rim	rim	rim	core	rim	core	rim	o-rim	core	rim
SiO_2	37.62	37.66	38.19	38.10	38.05	37.83	38.39	37.20	38.12	36.87	37.80	38.24	38.35	38.57	38.23	37.42	37.53	37.25	37.77	36.59	37.39	37.28
TiO_2	0.03	0.02	0.00	0.00	0.02	0.12	0.04	0.12	0.02	0.02	0.40	0.09	0.04	0.07	0.07	0.13	0.07	0.11	0.10	0.03	0.12	0.30
Al_2O_3	21.62	20.54	21.37	21.55	21.41	20.82	21.20	21.32	21.71	21.01	21.40	21.36	21.80	21.53	21.32	20.45	20.88	20.38	20.25	20.22	20.46	19.81
FeO[a]	28.64	28.37	27.02	26.80	28.01	29.79	27.29	27.00	27.97	29.70	26.31	28.57	28.66	28.57	28.31	24.16	26.29	26.17	27.13	18.67	24.62	24.08
MnO	0.21	2.39	0.29	0.25	0.32	0.19	0.83	1.13	0.28	1.27	0.64	0.75	0.79	0.75	0.39	5.98	3.58	6.21	3.44	15.28	6.54	2.57
MgO	4.48	1.82	5.78	6.32	5.50	1.62	3.42	1.27	3.99	4.21	3.99	3.74	5.91	5.11	3.49	1.43	2.31	0.93	1.40	0.94	0.14	0.17
CaO	7.60	9.76	6.89	6.52	6.70	9.99	9.51	12.13	8.88	5.87	9.68	8.17	5.19	6.21	8.55	10.07	8.78	8.64	9.57	7.66	11.27	15.15
Total	100.20	100.56	99.54	99.54	100.01	100.36	100.68	100.17	100.97	98.95	100.22	100.92	100.74	100.81	100.36	99.64	99.44	99.69	99.66	99.39	100.54	99.36
O = 12																						
Si	2.95	2.99	2.99	2.97	2.97	3.01	3.00	2.95	2.97	2.95	2.96	2.99	2.98	3.00	3.00	3.00	3.00	3.01	3.03	2.97	2.99	2.99
Ti	0.00	0.00	0.00	0.00	0.00	0.01	0.00	0.01	0.00	0.00	0.02	0.01	0.00	0.00	0.00	0.01	0.00	0.01	0.01	0.00	0.01	0.02
Al	2.00	1.92	1.97	1.98	1.97	1.95	1.96	1.99	1.99	1.98	1.97	1.97	1.99	1.97	1.98	1.93	1.97	1.94	1.92	1.93	1.93	1.87
Fe^{3+}	0.10	0.10	0.05	0.07	0.08	0.02	0.03	0.09	0.07	0.13	0.06	0.04	0.05	0.01	0.01	0.05	0.02	0.04	0.01	0.13	0.07	0.10
Fe^{2+}	1.77	1.78	1.72	1.68	1.75	1.96	1.76	1.70	1.75	1.86	1.66	1.82	1.81	1.85	1.85	1.57	1.73	1.73	1.81	1.14	1.57	1.51
Mn	0.01	0.16	0.02	0.02	0.02	0.01	0.05	0.08	0.02	0.09	0.04	0.05	0.05	0.05	0.03	0.41	0.24	0.42	0.23	1.05	0.44	0.17
Mg	0.52	0.22	0.67	0.73	0.64	0.19	0.40	0.15	0.46	0.50	0.47	0.44	0.68	0.59	0.41	0.17	0.28	0.11	0.17	0.11	0.02	0.02
Ca	0.64	0.83	0.58	0.54	0.56	0.85	0.80	1.03	0.74	0.50	0.81	0.68	0.43	0.52	0.72	0.86	0.75	0.75	0.82	0.67	0.97	1.30
Total	8.00	8.00	8.00	8.00	8.00	8.00	8.00	8.00	8.00	8.00	8.00	8.00	8.00	8.00	8.00	8.00	8.00	8.00	8.00	8.00	8.00	8.00

o-rim, outermost rim. Na (< 0.08 wt%), K (< 0.07 wt%) and Cr (< 0.05 wt%) contents are negligible.
[a]Total Fe as FeO.

Fig. 5a). The garnet of the eclogites displays prograde zoning, i.e. Mn (0.16–0.01 p.f.u.) decreases continuously from core to rim, and increases slightly at the outermost rim (0.02 p.f.u.), whereas Mg increases continuously from core (0.17 p.f.u.) to rim (0.75 p.f.u.), with slight decrease at the outermost rim (0.64 p.f.u.) (Fig. 5b,c). Fe^{2+} (1.78–2.01 p.f.u.) and Ca (0.96–1.04 p.f.u.) contents increase slightly from core to mantle, and then decrease continuously to the rim (Fe^{2+} = 1.69 p.f.u. and Ca = 0.55 p.f.u.). The X_{Fe} = Fe/(Fe + Mg) ratio is almost homogeneous from core to mantle, and then decreases towards the rim.

The composition of garnet in the garnet amphibolites varies within the range Mn = 0.02–0.08 p.f.u., Mg = 0.36–0.74 p.f.u., Ca = 0.44–0.91 p.f.u. and Fe^{2+} = 1.61–1.98 p.f.u (Table 1; Fig. 5a). Generally, Mg and Fe^{2+} increase and Ca decreases discontinuously from core to rim. Mn is relatively homogeneous. X_{Fe} continuously decreases from core to rim (0.81–0.72 p.f.u.). Atoll garnet is slightly richer in Mg and poorer in Ca than complete garnet (Fig. 5a).

The chemical compositions of the garnet vary slightly in the pelitic and granitic gneisses (Fig. 5a). Garnet in the pelitic gneisses has a composition of Mg (0.11–0.31 p.f.u.), Ca (0.52–0.82 p.f.u.), Fe^{2+} (0.83–0.94 p.f.u.) and Mn (0.13–0.88 p.f.u.). X_{Fe} continuously decreases from core to rim (0.94–0.86 p.f.u.). In the outermost rims of some garnet (e.g. sample 03–37) Mn contents are extremely high (up to 1.10 p.f.u.), with Mg = 0.12, Ca = 0.68 and Fe^{2+} = 1.05 p.f.u. Manganese enrichment at the rims of garnet is well documented (e.g. Tracy, 1982), and results from Mn diffusion during retrograde metamorphism. Garnet of the granitic gneiss has very low Mg contents (< 0.02 p.f.u.) with Fe^{2+} (1.50–1.57 p.f.u.), Mn (0.18–0.44) and Ca (0.97–1.30). X_{Fe} is homogeneous from core to rim (0.98–0.99 p.f.u.).

Clinopyroxene

Clinopyroxene in the eclogites is classified as omphacite and aegirine-augite (Morimoto, 1988) (Table 2; Fig. 6). Cpx1 inclusions in garnet are omphacite, and have been described by Orozbaev *et al.* (2007). Porphyroblastic Cpx2 is classified as omphacite, is zoned with increasing jadeite content from core ($Jd_{21}Aeg_{28}Aug_{51}$) to the mantle ($Jd_{50}Aeg_{14}Aug_{36}$) before decreasing slightly at the rim ($Jd_{42}Aeg_{15}Aug_{43}$). Some Cpx2 crystals are zoned, with jadeite contents decreasing from core ($Jd_{41}Aeg_{12}Aug_{47}$) to rim ($Jd_{23}Aeg_{16}Aug_{61}$). Cpx3 in the symplectite with Pl2 is omphacite and aegirine-augite, and jadeite contents vary from 9 to 20 mol%, whereas aegirine and augite contents range from 10 to 22 mol% and from 55 to 75 mol%, respectively.

Amphibole

Amphibole in the eclogites consists mainly of Na–Ca-amphibole and Ca-amphibole with minor Na-amphibole (Leake *et al.*, 1997) (Table 3; Fig. 7). Orozbaev *et al.* (2007) have already described Amp1 as inclusions in both garnet and Cpx2 of eclogites (glaucophane, Mg-taramite, Mg-katophorite, barroisite, taramite, winchite, actinolite and edenite). Amp2 in the matrix of the eclogites is zoned, with mainly Mg-taramite and rare taramite cores to Fe-pargasite or pargasite/Mg-hastingsite rims (Figs 3e & 7). Amp2 as a constituent of Amp2 + Pl2 has an Mg-taramite composition, whereas those replacing Cpx3 in

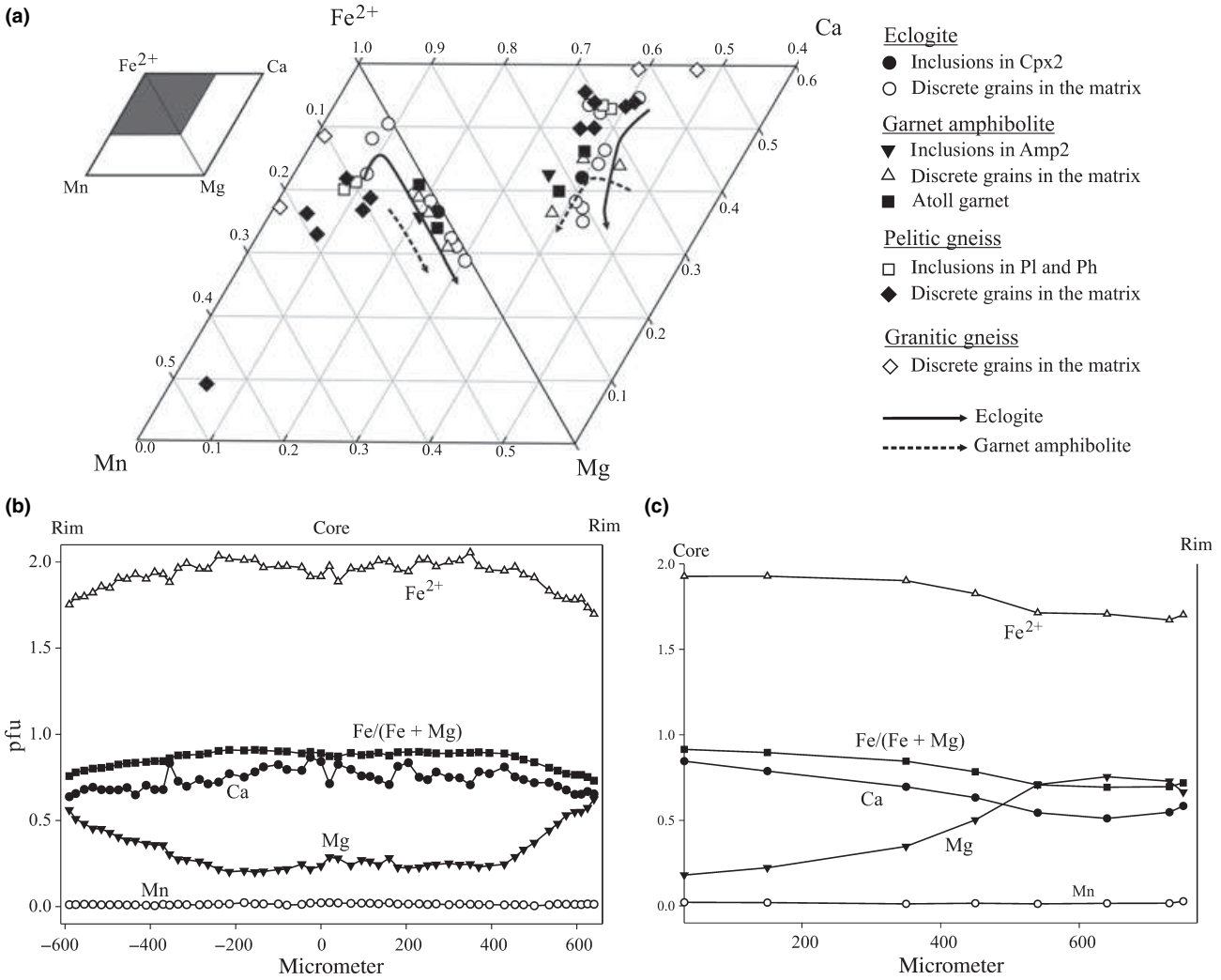

Fig. 5. (a) A Mn–Mg–Ca–Fe^{2+} diagram showing chemical composition of garnet; (b) and (c) chemical zoning pattern (rim–rim and core–rim) of garnet crystals from the eclogites.

symplectites of Cpx3 + Pl2 is Mg-hastingsite. Porphyroblastic Amp3 is zoned from Mg-taramite in the core to Mg-hastingsite or Fe-pargasite in the rim.

The ferric iron estimation for amphibole was performed as total cations 13 = Si + Al + Ti + Cr + Mg + Fe + Mn (for O = 23; 13eCNK method of Schumacher, in Leake *et al.*, 1997), which gives the maximum ferric iron estimate in amphibole. Applying the same method to amphibole in garnet amphibolites yields an unusual 'barroisite' composition with Si = 6.02–6.44 p.f.u., Na_B = (Na in the M4 site of amphibole) = 0.51–0.76, $(Na + K)_A$ = 0.14–0.36 and X_{Mg} = Mg/(Mg + Fe^{2+}) = 0.65–0.75 which does not fall within any of the amphibole nomenclature classifications proposed by Leake *et al.* (1997). Similar amphibole compositions were mentioned by Enami & Nagasaki (1999) from kyanite eclogites in the Sulu province (China). Nevertheless, the site assignment shown in fig. A-1 of Leake *et al.* (1997) makes it possible to define the limits of the stoichiometry of amphibole in garnet amphibolite, and all ferrous iron formulae calculated on the basis of 23 oxygen satisfy all six criteria [Si ≤ 8, ∑Ca ≤ 15 and ∑K ≤ 16 (minimum ferric iron) and ∑Al ≥ 8, ∑Mn ≥ 13 and ∑Na ≥ 15 (maximum ferric iron)]. Therefore, this offers no constraint on the ferric iron estimation, because there are no violations of the criteria Si ≤ 8, ∑Ca ≤ 15 and ∑K ≤ 16 (Leake *et al.*, 1997; Schumacher, 1991; Holland & Blundy, 1994). Amphibole in garnet amphibolites, taking all iron as Fe^{2+}, is classified as Mg-hornblende, edenite and pargasite/Fe-pargasite. Amp1 included within garnet is pargasite or Fe-pargasite. Amp2 in garnet amphibolites exhibits zoning from Mg-hornblende and/or edenite cores to pargasite/Fe-pargasite rims (Fig. 7). Amphibole included within porphyroblastic plagioclase in the pelitic gneisses is Mg-hornblende (samples KG-432).

Table 2. Representative compositions of clinopyroxene in eclogites.

Sample	KG-426							KG-427				03–18		
Mineral	Cpx1	Cpx1	Cpx2	Cpx2	Cpx2	Cpx3	Cpx3	Cpx1	Cpx2	Cpx2	Cpx3	Cpx1	Cpx2	Cpx3
Mode			core	mantle	rim				core	rim				
SiO_2	55.41	54.42	54.30	55.47	55.04	53.13	53.85	55.21	54.27	52.54	53.00	53.06	54.92	52.75
TiO_2	0.07	0.04	0.04	0.05	0.10	0.05	0.10	0.12	0.08	0.08	0.15	0.09	0.12	0.08
Al_2O_3	11.11	8.52	9.02	12.63	10.96	8.05	7.41	8.93	10.59	7.30	6.05	8.80	10.29	5.58
FeO[a]	8.14	11.23	10.51	6.17	7.40	10.10	8.36	8.48	7.94	10.27	10.25	11.46	8.37	10.41
MnO	0.06	0.08	0.01	0.05	0.06	0.06	0.02	0.00	0.00	0.02	0.11	0.13	0.08	0.06
MgO	6.29	6.23	6.06	5.89	6.55	7.94	8.79	8.00	6.68	8.09	8.91	6.51	6.38	8.72
CaO	10.42	11.38	10.34	9.40	11.20	15.00	15.32	13.29	11.95	15.61	16.40	13.68	11.73	16.65
Na_2O	8.29	7.69	8.57	9.33	8.27	5.29	5.67	6.46	7.62	5.51	5.02	6.67	7.36	4.48
Total	99.79	99.59	98.85	98.99	99.58	99.62	99.52	100.49	99.13	99.42	99.89	100.40	99.25	98.73
O = 6														
Si	1.98	1.97	1.97	1.97	1.96	1.94	1.95	1.98	1.96	1.92	1.94	1.92	1.99	1.96
Ti	0.00	0.00	0.00	0.00	0.00	0.00	0.00	0.00	0.00	0.00	0.00	0.00	0.00	0.00
Al	0.47	0.36	0.38	0.53	0.46	0.35	0.32	0.38	0.45	0.31	0.26	0.38	0.44	0.24
Fe^{3+}	0.15	0.23	0.28	0.17	0.18	0.14	0.17	0.11	0.17	0.22	0.21	0.25	0.10	0.15
Fe^{2+}	0.10	0.11	0.04	0.01	0.04	0.17	0.09	0.15	0.07	0.09	0.10	0.10	0.16	0.17
Mn	0.00	0.00	0.00	0.00	0.00	0.00	0.00	0.00	0.00	0.00	0.00	0.00	0.00	0.00
Mg	0.33	0.34	0.33	0.31	0.35	0.43	0.48	0.43	0.36	0.44	0.49	0.35	0.34	0.48
Ca	0.40	0.44	0.40	0.36	0.43	0.59	0.60	0.51	0.46	0.61	0.64	0.53	0.45	0.66
Na	0.57	0.54	0.60	0.64	0.57	0.38	0.40	0.45	0.53	0.39	0.36	0.47	0.52	0.32
Total	4.00	4.00	4.00	4.00	4.00	4.00	4.00	4.00	4.00	4.00	4.00	4.00	4.00	4.00

K (< 0.05 wt%) and Cr (< 0.08 wt%) contents are negligible.
[a]Total Fe as FeO.

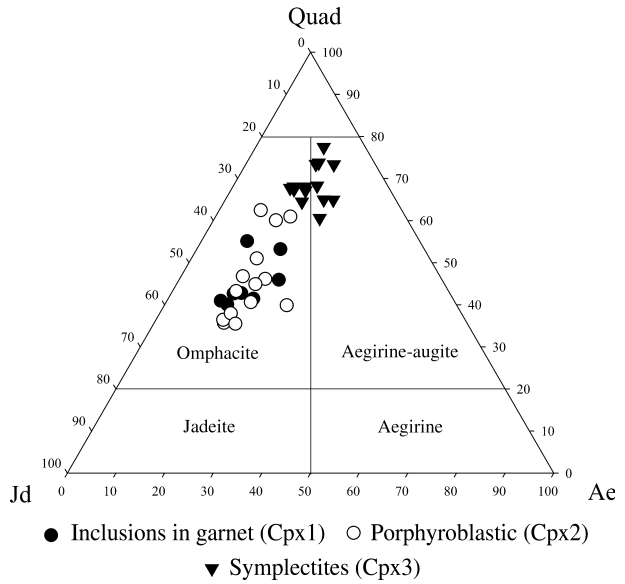

Fig. 6. Chemical compositions of clinopyroxene.

White mica

Compositions of Ph1 and Pg1 inclusions in garnet of the eclogites have been already described by Orozbaev *et al*. (2007). Ph2 in the eclogites is zoned from core to rim, with Si decreasing from 6.66–6.79 to 6.15–6.30 p.f.u. (O = 22) and X_{Na} = Na/(Na + K) increasing from 0.03–0.11 to 0.15–0.21 (Table 4; Fig. 8). Occasionally, the outermost rims of Ph2 have Ms composition (Si = 5.96–6.09 p.f.u., X_{Na} = 0.25–0.38) (Fig. 8). Pg2 in the matrix has Si contents of 5.81–5.95 p.f.u. and X_{Na} of 0.83–0.94, with a small amount of the margarite component (Ca = 0.02–0.04 p.f.u.).

Ph1 included within garnet and porphyroblastic plagioclase in the pelitic gneisses has Si content ranging from 6.29 to 6.69 p.f.u. with X_{Na} = 0.03–0.09. Ph1 inclusions in zircon separated from both the pelitic and granitic gneisses has Si contents of 6.63–6.85 p.f.u. (X_{Na} = 0.01–0.04) and 6.26–6.88 p.f.u. (X_{Na} = 0.01–0.03), respectively. Si contents in Ph2 in the matrix of the pelitic gneisses range from 6.29 and 6.67 p.f.u. (X_{Na} = 0.06–0.08), and decrease from core to rim.

Feldspar

The composition of Pl1 ($An_{4–16}$) in the eclogites has already been described by Orozbaev *et al*. (2007). Pl2 in the eclogites is zoned from albite in the cores ($An_{3–9}$) to oligoclase in the rims ($An_{10–21}$). Pl2 as a constituent of symplectite after omphacite is albite ($An_{2–9}$). Pl2 replacing the rims of garnet has a composition of $An_{5–13}$, whereas Pl3 in symplectite consisting of biotite after phengite is oligoclase ($An_{11–22}$). K-feldspar ($Or_{97–98}$) occasionally occurs as inclusions in garnet of the eclogites.

In the garnet amphibolites, feldspar replacing amphibole in the interior of atoll garnet is oligoclase ($An_{12–18}$) and K-feldspar ($Or_{98–99}$). In the pelitic gneisses, the anorthite content of plagioclase increases from cores (An_1) to rims (An_{16}). Feldspar in the granitic gneisses is albite ($An_{0–5}$) and K-feldspar ($Or_{92–97}$).

Other minerals

The $X_{Ps} = Fe^{3+}/(Al + Fe^{3+})$ content of Ep1 included within garnet in the eclogites ranges from

Table 3. Representative compositions of amphibole.

Rock type	Eclogite											Garnet amphibolite					Pelitic gneiss
Sample	KG-426				KG-427			03–18				03–17					KG-432
Mineral	Amp1	Amp2	Amp2	Amp2	Amp2	Amp2	Amp3	Amp2	Amp2	Amp3	Amp3	Amp1	Amp2	Amp2	Amp2	Amp2	Amp
Mode										core	rim		core	rim	rim	rim	inc
SiO_2	44.47	40.92	42.11	39.68	40.89	40.23	41.56	41.25	40.79	43.43	39.66	43.94	44.37	42.67	42.75	43.06	49.88
TiO_2	0.61	0.10	0.44	0.07	0.91	0.33	0.66	0.63	0.36	0.75	0.54	0.45	0.40	0.52	0.65	0.61	0.02
Al_2O_3	14.07	14.77	15.23	13.70	15.00	13.56	14.92	14.26	12.53	14.07	15.56	15.58	12.42	14.90	15.24	15.06	4.05
FeO[a]	14.48	18.73	14.65	21.21	16.15	17.22	14.52	17.65	18.72	16.79	18.91	14.05	16.71	15.82	16.04	16.86	16.18
MnO	0.03	0.00	0.04	0.10	0.06	0.12	0.03	0.14	0.20	0.11	0.14	0.07	0.29	0.17	0.20	0.21	0.82
MgO	9.80	8.54	10.10	8.05	8.82	9.72	10.29	8.30	9.00	8.79	7.61	10.76	11.74	9.64	9.74	8.89	12.54
CaO	7.47	8.80	8.25	9.94	9.11	10.35	9.54	9.13	10.26	7.97	10.02	9.58	8.36	9.41	8.34	9.01	11.41
Na_2O	4.91	4.42	4.78	3.57	3.98	3.37	3.92	3.63	2.82	4.31	3.39	2.73	2.35	2.90	3.29	2.94	1.19
K_2O	0.74	0.99	0.85	1.53	1.27	1.13	1.28	1.07	1.46	0.64	1.54	0.25	0.23	0.31	0.30	0.34	0.38
Total	96.58	97.27	96.45	97.85	96.19	96.03	96.72	96.06	96.14	96.86	97.37	97.41	96.87	96.34	96.55	96.98	96.47
O = 23																	
Si	6.55	6.13	6.24	6.02	6.18	6.12	6.20	6.25	6.23	6.43	6.02	6.44	6.61	6.40	6.39	6.43	7.40
Ti	0.07	0.01	0.05	0.01	0.10	0.04	0.07	0.07	0.04	0.08	0.06	0.05	0.05	0.06	0.07	0.07	0.00
Al	2.44	2.61	2.66	2.45	2.67	2.43	2.62	2.55	2.26	2.45	2.78	2.69	2.18	2.64	2.69	2.65	0.71
Fe^{3+}	0.42	0.82	0.61	0.92	0.39	0.66	0.40	0.57	0.71	0.64	0.51	0.00	0.00	0.00	0.00	0.00	0.44
Fe^{2+}	1.36	1.53	1.21	1.77	1.66	1.53	1.41	1.66	1.68	1.44	1.89	1.72	2.08	1.98	2.01	2.11	1.57
Mn	0.00	0.00	0.00	0.01	0.01	0.02	0.00	0.02	0.03	0.01	0.02	0.01	0.04	0.02	0.03	0.03	0.10
Mg	2.15	1.91	2.23	1.82	1.99	2.20	2.29	1.87	2.05	1.94	1.72	2.35	2.61	2.16	2.17	1.98	2.77
Ca	1.18	1.41	1.31	1.61	1.48	1.69	1.53	1.48	1.68	1.26	1.63	1.50	1.33	1.51	1.34	1.44	1.81
Na	1.40	1.28	1.37	1.05	1.17	0.99	1.13	1.07	0.84	1.24	1.00	0.78	0.68	0.84	0.95	0.85	0.34
K	0.14	0.19	0.16	0.30	0.25	0.22	0.24	0.21	0.28	0.12	0.30	0.05	0.04	0.06	0.06	0.06	0.07
Total	15.72	15.88	15.84	15.96	15.89	15.90	15.90	15.75	15.80	15.62	15.92	15.58	15.62	15.67	15.70	15.63	15.23

inc, inclusions in porphyroblastic plagioclase. Cr contents of analysed amphibole in eclogite, garnet amphibolite and pelitic gneisses are negligible (< 0.06 wt%).
[a]Total Fe as FeO.

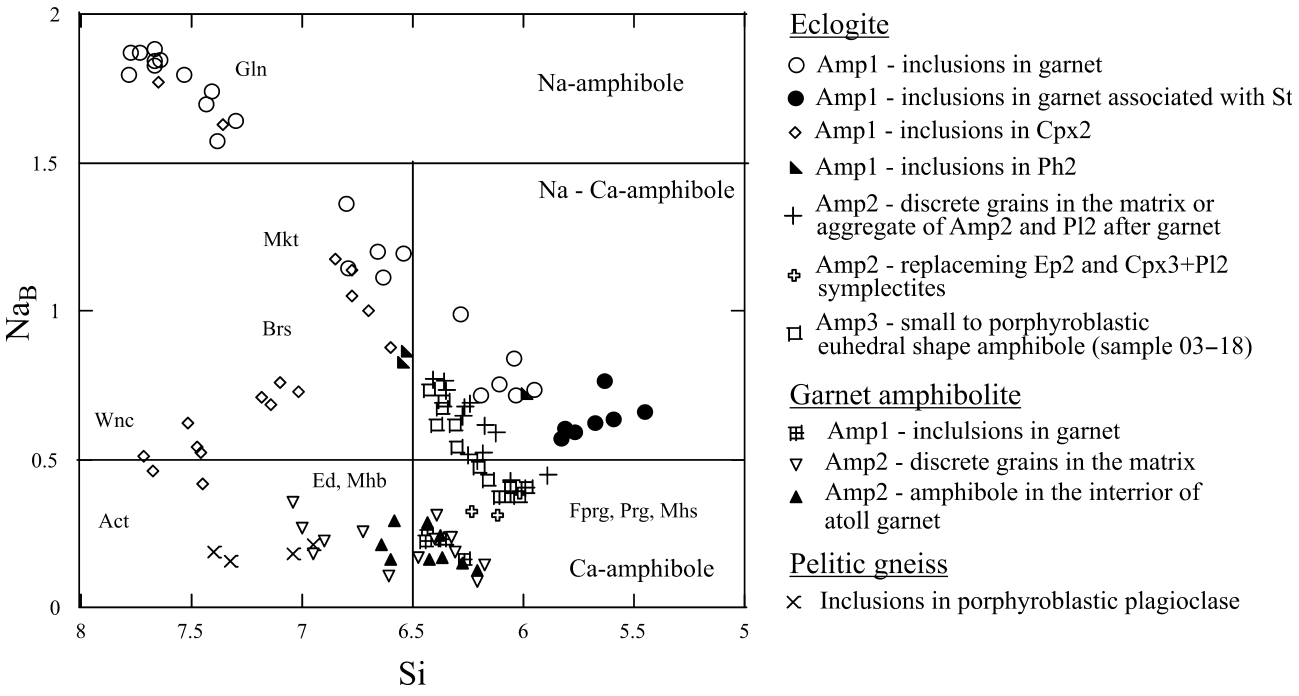

Fig. 7. Chemical compositions of amphibole. Amp1 compositions from Orozbaev *et al.* (2007) are also included.

0.19 to 0.23. Ep2 in the matrix of the eclogites has X_{Ps} = 0.17–0.22. Ep1 and Ep2 in the country rock gneisses have X_{Ps} of 0.18–0.28 and 0.24–0.28, respectively. Ep2 in both the eclogites and the country rock gneisses is occasionally zoned, from REE-bearing cores to REE-free rims. X_{Mg} = Mg/(Fe + Mg)

Table 4. Representative compositions of mica and chlorite.

Rock type	Eclogite									Garnet amphibolite		Pelitic gneiss									
Sample	KG-426					KG-427		03–18		03–17		KG-432				KG-430				03–37	
Mineral	Ph2	Ph2	Ph2	Ph2	Pg2	Ph2	Ph2	Ph2	Ph2	Chl	Bt	Ph1	Ph2	Chl	Bt2	Ph1	Ph2	Ph2	Bt2	Ph2	Bt2
Mode	core	core	mantle	o-rim		core	rim	core	rim								core	rim			
SiO_2	48.34	48.21	48.23	43.39	45.18	48.40	45.84	48.79	46.69	25.80	35.83	47.31	46.78	38.05	36.37	45.99	46.82	45.38	36.35	46.32	36.24
TiO_2	0.26	0.28	0.66	0.12	0.12	0.25	1.02	0.38	0.77	0.14	0.83	0.88	0.93	0.80	1.74	0.87	1.19	1.22	2.57	1.14	2.41
Al_2O_3	27.17	26.56	30.94	36.17	39.27	27.15	29.60	27.11	28.92	21.13	17.44	24.75	24.48	14.09	13.82	30.52	27.39	29.21	15.95	27.11	15.53
Cr_2O_3	0.00	0.00	0.00	0.01	0.00	0.00	0.00	0.00	0.03	0.07	0.02	0.00	0.00	0.00	0.00	0.00	0.01	0.01	0.00	0.01	0.00
FeO[a]	2.88	2.85	1.98	1.69	0.74	3.36	3.48	4.16	4.16	19.81	19.20	6.38	6.14	15.81	16.79	4.69	4.31	5.67	18.55	6.42	22.28
MnO	0.00	0.00	0.00	0.00	0.00	0.00	0.01	0.00	0.00	0.14	0.11	0.08	0.05	0.58	0.63	0.13	0.08	0.08	0.39	0.04	0.47
MgO	3.27	3.30	2.30	0.37	0.18	3.04	2.22	2.96	2.46	19.21	11.14	2.80	2.72	13.93	12.86	1.69	2.36	1.95	10.81	2.02	9.42
CaO	0.00	0.00	0.02	0.00	0.21	0.00	0.05	0.00	0.03	0.02	0.03	0.04	0.00	0.02	0.00	0.04	0.00	0.07	0.02	0.00	0.09
Na_2O	0.72	0.46	1.11	2.25	6.93	0.53	0.72	0.63	0.41	0.03	0.08	0.28	0.31	0.18	0.05	0.30	0.43	0.39	0.08	0.28	0.07
K_2O	10.37	10.68	9.43	8.26	1.03	10.26	9.78	10.01	10.29	0.04	9.38	9.54	10.09	9.04	9.19	10.74	10.48	10.11	9.51	10.72	9.06
Total	93.01	92.34	94.67	92.26	93.66	92.99	92.72	94.04	93.76	86.39	94.06	92.06	91.50	92.50	91.45	94.97	93.07	94.09	94.23	94.06	95.57
O	22	22	22	22	22	22	22	22	22	28	22	22	22	28	22	22	22	22	22	22	22
Si	6.66	6.70	6.46	5.95	5.90	6.67	6.35	6.67	6.43	5.36	5.53	6.69	6.67	5.87	5.74	6.29	6.51	6.29	5.60	6.46	5.59
Ti	0.03	0.03	0.07	0.01	0.01	0.03	0.11	0.04	0.08	0.02	0.10	0.09	0.10	0.09	0.21	0.09	0.12	0.13	0.30	0.12	0.28
Al	4.41	4.35	4.88	5.85	6.04	4.41	4.83	4.37	4.69	5.18	3.17	4.12	4.12	2.56	2.57	4.92	4.49	4.77	2.89	4.45	2.82
Cr	0.00	0.00	0.00	0.00	0.00	0.00	0.00	0.00	0.00	0.01	0.00	0.00	0.00	0.00	0.00	0.00	0.00	0.00	0.00	0.00	0.00
Fe^{2+}	0.33	0.33	0.22	0.19	0.08	0.39	0.40	0.48	0.48	3.45	2.48	0.75	0.73	2.04	2.22	0.54	0.50	0.66	2.39	0.75	2.88
Mn	0.00	0.00	0.00	0.00	0.00	0.00	0.00	0.00	0.00	0.02	0.01	0.01	0.01	0.08	0.08	0.02	0.01	0.01	0.05	0.00	0.06
Mg	0.67	0.68	0.46	0.07	0.04	0.63	0.46	0.60	0.50	5.96	2.56	0.59	0.58	3.20	3.02	0.34	0.49	0.40	2.48	0.42	2.17
Ca	0.00	0.00	0.00	0.00	0.03	0.00	0.01	0.00	0.00	0.01	0.00	0.01	0.00	0.00	0.00	0.01	0.00	0.01	0.00	0.00	0.01
Na	0.19	0.12	0.29	0.60	1.75	0.14	0.19	0.17	0.11	0.01	0.02	0.08	0.08	0.05	0.02	0.08	0.11	0.10	0.02	0.07	0.02
K	1.82	1.89	1.61	1.45	0.17	1.81	1.73	1.74	1.81	0.01	1.85	1.72	1.84	1.78	1.85	1.87	1.86	1.79	1.87	1.91	1.78
Total	14.11	14.11	13.98	14.13	14.03	14.07	14.09	14.06	14.10	20.03	15.72	14.06	14.13	15.67	15.70	14.14	14.10	14.15	15.60	14.19	15.62

o-rim, outermost rim.
[a]Total Fe as FeO.

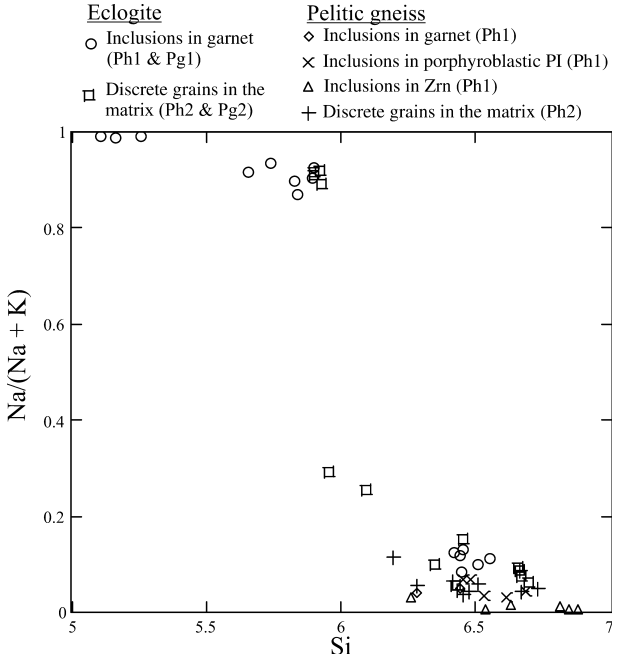

Fig. 8. Chemical compositions of white mica.

of chlorite in the eclogites and country rock gneisses varies from 0.35 to 0.50 and from 0.52 to 0.66, respectively.

P–T EVOLUTION OF THE HIGH-*P* METAMORPHIC ROCKS

The textural relationship among minerals and the mineral chemistry of the eclogites in the Aktyuz Formation record three distinct metamorphic events, i.e. a first MP–HT metamorphism; a second HP–LT metamorphism; and a third medium- to HP–HT metamorphism (Fig. 9). In contrast, the garnet amphibolites and country rock gneisses record a single metamorphic event.

THERMOCALC v.3.21 (Powell & Holland, 1994) with an updated internally consistent thermodynamic data set (Holland & Powell, 1998) was used to apply an 'average *P–T*' mode calculation for the mineral assemblages that are interpreted to have equilibrated in each stage of the evolution of the Aktyuz HP metamorphic rocks. The activities of the minerals were calculated using the AX program (Holland & Powell, 1998). End-members with very low activities (< 0.0001) were excluded from the calculation. If fit indices exceeded the value allowable for 95% confidence in the *P–T* result, then the most suspect activity (largest e*) was removed and the calculation was re-run (Dale & Holland, 2003). The activity of H_2O is assumed to be unity. Quartz and H_2O are present in all assemblages. Independent reactions used for the THERMOCALC calculations are listed in Table 5. Additionally, the available geothermobarometers have been applied for the estimation of *P–T* conditions.

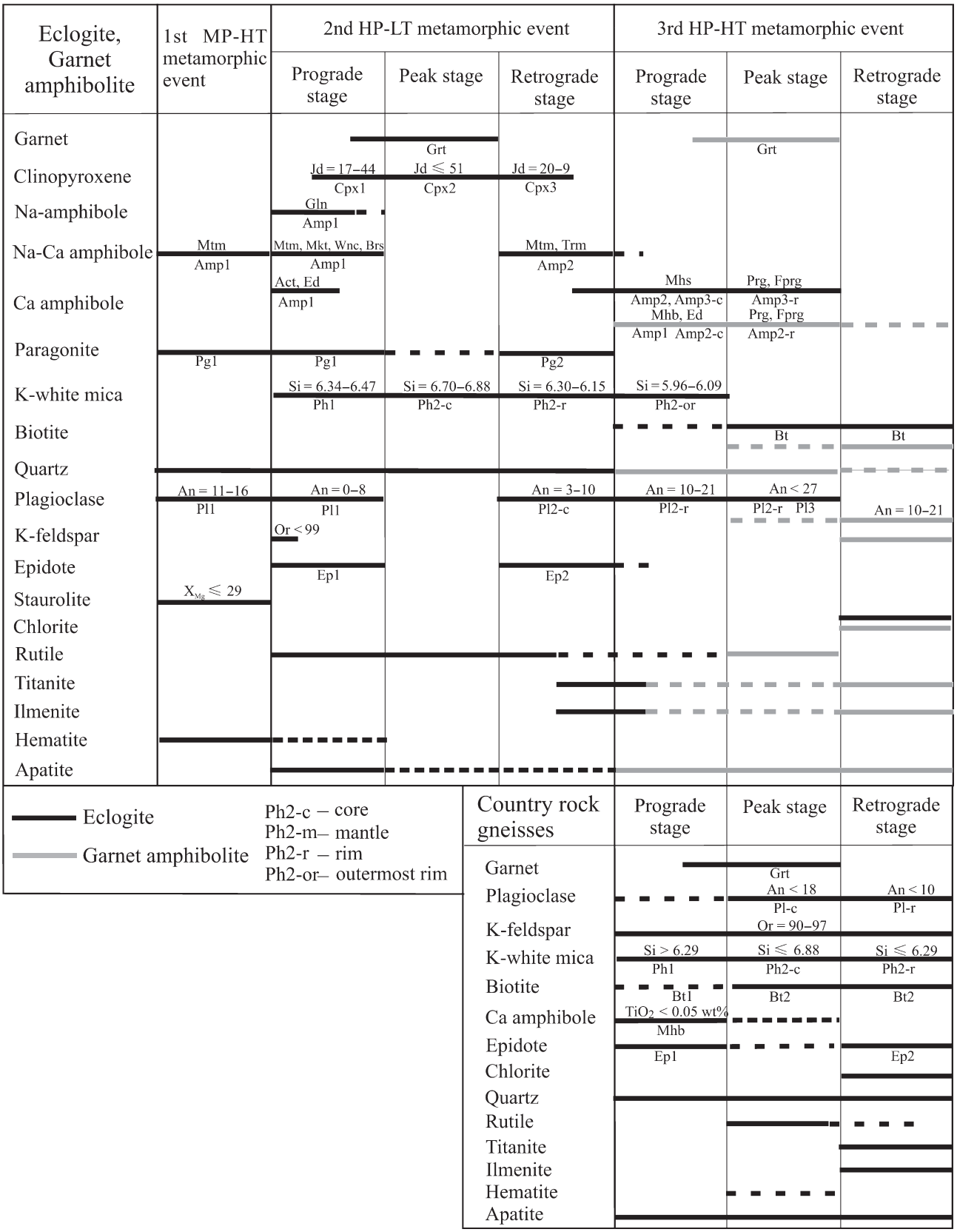

Fig. 9. Polyphase metamorphic evolution and paragenesis of the Aktyuz HP metamorphic rocks.

Table 5. List of independent reactions used in THERMOCALC 'average *P–T* mode' calculations.

	Reactions
For eclogites	
1	py + 2gr + 3cel = 6di + 3mu
2	3hed + 2pa = gr + alm + 2jd + 2q + $2H_2O$
3	4pa + 3cel = py + 4jd + 3mu + 4q + $4H_2O$
4	py + 3hed = alm + 3di
5	jd + q = ab
6	2di + ts + 2q = tr + 2an
7	2di + ts + 2ab = 2jd + tr + 2an
8	2parg + 6ab = 8jd + tr + ts
9	ts + 2cel = tr + 2mu
10	2tr + 5parg + 18an + 6pa = 11jd + 10ts + 6cz
11	cz + fep = 2ep
12	jd + ep = acm + cz
13	5parg + 22ab + 6cz = 27jd + 4tr + 14an + $4H_2O$
14	4pa + 12an + 3tr + 6jd = 10ab + 4cz + 5ts
15	4pa + 12an + 2cz + 3tr + 6acm = 10ab + 6ep + 5ts
16	5pa + 10cel + 8an + 4acm = 10mu + 9ab + 2fep + 2tr + $2H_2O$
17	18di + 2ts + 6pa = 5jd + 4tr + parg + 6cz
18	11parg + 26ab + 6cz = 14di + 37jd + 10ts + $4H_2O$
19	acm + cz + q = ab + ep
For garnet amphibolite	
20	5py + 3fact = 5alm + 3tr
21	12parg + 36q = 2py + 4gr + 3tr + 3ts + 6gl
22	42parg + 114q = 20py + 22gr + 9tr + 21gl + $12H_2O$
23	5alm + 12parg + 36q = 7py + 4gr + 3fact + 3ts + 6gl
24	78fact + 105ts = 80gr + 130alm + 63tr + 120q + $120H_2O$
25	3fact + 21ts = 21py + 16gr + 5alm + 24q + $24H_2O$
For country rock gneisses	
26	3tr + 18an + 4mu + 3phl = 8ts + 7san + 4cz
27	5ts + 4san + 4cz + 6q = 3tr + 12an + 4mu
28	tr + 3ts + 7cel = 4cz + 7phl + 21q + $2H_2O$
29	6an + 12cel + phl = 3tr + 7san + 6mu + $4H_2O$
30	2parg + 8q = tr + ts + 2ab
31	4cz + 5ann + 16q = 3fact + 2an + san + 4mu
32	3ts + 4parg + 4cz + 22q = 5tr + 12an + 4pa
33	8ep + 5ann + 16q = 3fact + 2an + san + 4mu + 4fep
34	2pa + 3cel = 2ab + 2mu + phl + 3q + $2H_2O$
35	ab + 2mu + 2cz + phl + 5q = 4an + pa + 3cel
36	2mu + 8ep + phl + 7q = 8an + 3cel + 4fep + $2H_2O$
37	2phl + mu + 6q = py + 3cel
38	py + gr + mu = phl + 3an
39	gr + alm + mu = ann + 3an
40	py + 3ann + 2pa + 9q = 3alm + 2ab + 3cel + $2H_2O$
41	3east + 6q = py + phl + 2mu
42	phl + east + 6q = py + 2cel

Mineral abbreviations after Holland & Powell (1998).

The results of all *P–T* estimates are summarized in Table 6.

Metamorphism of eclogites and garnet amphibolites

First MP–HT metamorphic event (M1)

This first metamorphic event of the amphibolite/epidote-amphibolite facies conditions (560–650 °C and 4–10 kbar) in the Aktyuz eclogites has been described by Orozbaev *et al*. (2007). They reported relict mineral assemblages of polyphase inclusions in the cores and mantles of simple prograde zoned garnet, i.e. Mg-taramite + Fe-staurolite ($X_{Mg} < 0.29$) + paragonite ± oligoclase ($An_{<16}$) ± hematite. Notably, the same garnet grain contains also inclusions of glaucophane, barroisite, epidote and paragonite. They interpreted that the Fe-rich staurolite along with Mg-taramite, paragonite and oligoclase relict inclusions in garnet were formed during a relatively MP–HT metamorphic event of amphibolite facies conditions (M1) before the epidote-blueschist facies conditions of eclogitic metamorphic event (M2) was attained.

Second high-pressure metamorphic event (M2)

Orozbaev *et al*. (2007) reported Na-amphibole (glaucophane) and Na–Ca-amphibole (Mg-katophorite, Mg-taramite and barroisite), aegirine-rich clinopyroxene, paragonite, phengite, epidote, albite, quartz, rutile and hematite inclusions in the cores and rims of garnet. They suggested that these phases formed during the prograde stage of the epidote-blueschist facies (330–570 °C; 8–16 kbar; M2-E1) before the eclogite facies conditions (M2-E2) of the second HP metamorphic event (M2). The peak metamorphic assemblage of Grt + Omp + Ph + Qz + Rt ± Pg was stable in the eclogite facies conditions of 600–710 °C and 15–25 kbar (Orozbaev *et al*., 2007) (Fig. 10a).

In this study, THERMOCALC calculations have been applied for the peak metamorphic assemblage. In these calculations, the chemical compositions used were the garnet rims (with highest Mg and lowest X_{Fe} contents), omphacite inclusions (Jd = 30–44) in the rim of garnet, and core compositions of matrix phengite (Ph2), assuming that the Ph2 cores, containing inclusions of garnet and Cpx2, with highest Si content (6.66–6.79 p.f.u.) were formed during the peak metamorphic conditions. The outermost rim of some garnet reflected by diffusional resetting (Fig. 5c) has not been used in the calculation, instead, garnet free of diffusional affects (Fig. 5b) is applied. The *P–T* conditions estimated for the eclogite facies stage (M2-E2) are 575–645 °C and 21–23 kbar (Fig. 10a). Consistent *P–T* estimation was also obtained using the Grt-Ph-Cpx geothermobarometer (Ravna & Terry, 2004). The GCPKS spreadsheet application gives the intersects of the Grt-Ph-Cpx geobarometer (Ravna & Terry, 2004) and Grt-Cpx geothermometer (Ravna, 2000) curves at conditions of 550–660 °C and 21–23 kbar. The temperatures estimated by the geothermometers of Ellis & Green (1979) and Powell (1985) are ~50 °C greater. The estimated pressure conditions of 21–23 kbar are consistent with those of previous studies (15–25 kbar) and lie below the paragonite-out reaction of Pg = Jd + Ky + H_2O (Holland, 1979), whereas the estimated temperature of 550–660 °C is lower than the 600–710 °C estimate of Orozbaev *et al*. (2007). This difference is mainly caused by different calibration of the Grt-Cpx geothermometers applied in this study (Ravna, 2000), v. those of Ellis & Green (1979) and Powell (1985) in the previous study. We have applied Ravna (2000), which is based on both experimental and natural data sets, and incorporates the effect of Mn content of garnet on the K_D value, and thus supersedes the previous calibrations.

The retrograde stage of the eclogites (M2-E3) is represented by omphacite breakdown to symplectite

Table 6. Summary of the estimated *P–T* conditions for the Aktyuz HP metamorphic rocks.

Rock type	Sample	Stage	Mineral assemblage	Reactions	THERMOCALC						GCPKS, RT04		GP84
					T, °C	*T*, sd	*P*, kbar	*P*, sd	cor	sigfit	*T*, °C	*P*, kbar	*T*, °C
Eclogite	KG-426	Peak	Grt, Cpx1, Ph2-c	2, 3, 4	617	52	23.3	2.6	−0.474	0.24	612	23.1	
		Peak	Grt, Cpx1, Ph2-c	1, 2, 3	643	56	22.9	2.7	−0.389	0.69	663	23.6	
		Retrograde	Cpx3, Pl2, Amp2	5, 6, 7, 8	544	63	10.5	1.0		0.30			
		Retrograde	Cpx3, Pl2, Amp2, Ep2, Ph2-m	5, 8, 9, 10, 11, 12, 13	561	55	11.2	1.7	0.922	1.27			
	KG-427	Peak	Grt, Cpx1, Ph2-c	1, 2, 3	595	52	21.2	2.4	−0.348	0.44	590	22.8	
		Retrograde	Cpx3, Pl2, Amp2, Ep2, Ph2-m	5, 9, 10, 11, 14, 15, 16	555	59	10.2	1.8	0.928	1.28			
	03–18	Peak	Grt, Cpx1, Ph2-c	1, 2, 3	574	52	22.7	2.4	−0.378	0.10	548	21.4	
		Retrograde	Cpx3, Pl2, Amp2, Ep2, Ph2-m	5, 6, 8, 9, 17, 18, 19	564	46	10.3	1.4	0.927	0.76			
Grt-amph	03–17	Prograde	Grt, Amp2	20, 21, 22	633	123	11.3	3.6	0.553	1.72			601
		Prograde	Grt-m, Amp1	21, 22, 23	638	69	12.5	1.9	0.385	0.82			601
		Peak	Grt-r, Amp2-r	21, 22, 24	737	83	15.2	2.3	0.506	0.11			693
		Peak	Grt-r, Amp2-r	20, 21, 22	675	72	14.6	2.1	0.554	0.58			676
		Peak	Grt-r, Amp2-r	20, 21, 25	712	106	15.2	2.5	0.619	0.69			677
Pelitic gneiss	KG-432	Prograde	Amp, Pl-c, Ep1, Ph1, Kfs, Bt1	26, 27, 28, 29, 30, 31, 32, 33	477	77	9.6	3.2	0.939	1.36			
		Peak	Pl-r, Ph2-c, Ep2, Bt2	34, 35, 36	637	126	12.8	4.5	0.987	0.51			
	KG-430	Peak	Grt-r, Pl, Ph2-c, Bt2	37, 38, 39, 40	745	67	15.0	2.4	0.810	1.62			
		Peak	Grt-r, Pl, Ph2-c, Bt2	38, 39, 40, 41, 42	711	53	13.9	1.9	0.796	1.44			
	03–37	Peak	Grt-r, Pl, Ph2-c, Bt2	37, 38, 39, 40, 41	736	61	14.1	1.9	0.774	1.36			
		Peak	Grt-r, Pl, Ph2-c, Bt2	37, 38, 39, 40, 41	725	47	14.6	1.6	0.787	1.13			
		Peak	Grt-r, Pl, Ph2-c, Bt2	37, 38, 39, 40, 41	737	69	13.8	2.1	0.807	1.42			

GCPKS, RT04, Grt-Cpx-Ph-Ky-Qz/Coe geothermobarometer (Ravna & Terry, 2004);
GP84, Grt-Hbl geothermometer (Graham & Powell, 1984).

consisting of Cpx3 ($Jd_{9–20}$) and albite (Pl2; $An_{2–9}$), and garnet is replaced by Mg-taramite or aggregate of Mg-taramite and Pl2 ($An_{5–13}$) (Fig. 3a,b). Furthermore, symplectites consisting of Cpx3 and albite (Pl2) coexist with Mg-taramite (Amp2), epidote, and phengite (Si < 6.5) in the retrograded portions of the eclogites (Fig. 3c), indicating a retrograde mineral assemblage of the epidote-amphibolite facies conditions. These suggest a representative mineral assemblage of Cpx3 ($Jd_{9–20}$), Pl2 ($An_{2–13}$), Na∼Ca-amphibole, phengite and epidote. Based on the mineral textures of these retrograded minerals (Fig. 3b,c), it is assumed that local equilibrium has been reached, and their rim-rim composition are applied for the geothermobarometric calculation. The *P–T* estimation of the retrograde stage in eclogites using THERMOCALC yielded 545–565 °C and 10–11 kbar (Fig. 10a). The estimated minimum pressure of 10 kbar at 550 °C is also suggested by low contents (Jd = 9) in Cpx3 + Pl2 symplectites (Holland, 1983). As prograde and/or retrograde metamorphism is a dynamic evolution with changing *P* and *T*, the estimated *P–T* conditions for this stage represent an arrested point during the retrograde *P–T* path of the Aktyuz eclogites.

Combining the prograde metamorphism of the epidote-blueschist facies conditions (M2-E1) with the peak metamorphic conditions of the eclogite facies (M2-E2) and subsequent retrograde metamorphism of the epidote-amphibolite facies (M2-E3) suggests a clockwise *P–T* path for the second HP metamorphic event (M2) in the Aktyuz eclogites (Fig. 10a).

Third HP–HT metamorphic event (M3)

The constraint on the third metamorphic event (M3) is obtained from garnet amphibolites which occur in the margins of the amphibolite-eclogite body. These were strongly affected by the third high-*P* and high-*T* metamorphism (M3) after the second HP metamorphic event (M2).

Garnet in garnet amphibolites has prograde zoning (Fig. 5a), suggesting that it formed during the prograde third HP–HT metamorphic event (M3). Garnet in garnet amphibolite contains inclusions of pargasite, quartz and rutile (Fig. 4b). The composition of garnet mantles (Mg > 0.36 p.f.u., X_{Fe} < 0.81 p.f.u.) and pargasite inclusions suggest conditions of 630–640 °C and 11–12 kbar for the prograde stage (M3-G1) just prior to peak metamorphic conditions (M3-G2; Fig. 10b). Phengite is apparently absent from the garnet amphibolites. Amp2 in the matrix of the garnet amphibolites shows prograde zoning from Mg-hornblende and edenite cores to Fe-pargasite or pargasite rims (Fig. 7). The peak metamorphic conditions (M3-G2) of the garnet amphibolites estimated using the mineral rim–rim compositions of the garnet (Mg < 0.70 p.f.u.; X_{Fe} > 0.72 p.f.u.) and pargasite assemblage, and THERMOCALC calculation yielded 675–735 °C and 14–15 kbar (Fig. 10b). The Grt-Amp geothermometer (Graham & Powell, 1984) yields similar temperature estimates of 600 and 675–695 °C for the prograde and peak stages, respectively (Table 6). The higher pressure estimate for the garnet amphibolites is also supported by total Al_2O_3 content (12.0–15.5 wt%) of Amp2, using a semiquantitative thermobarometer of Ernst & Liu (1998). Although the estimated *P–T* conditions suggest eclogite facies conditions, clinopyroxene was not produced in the garnet amphibolites during the peak metamorphic conditions of the third metamorphic event. Ernst & Liu (1998) suggested that the plagioclase-out boundary in the hydrous MORB system does not represent the

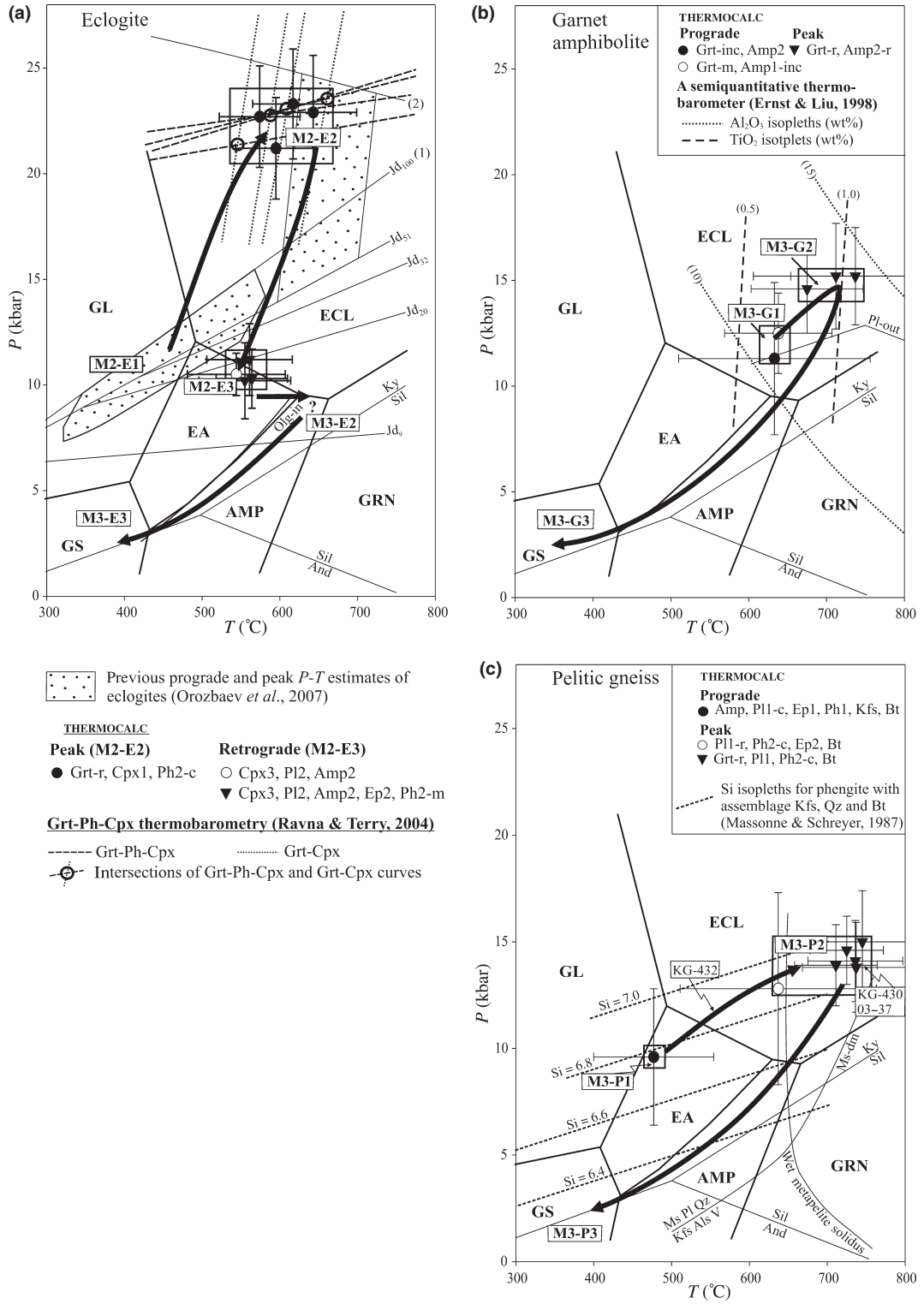

Fig. 10. Estimated *P–T* conditions for Aktyuz HP metamorphic rocks (*P–T* boundary after Takasu, 1989). ECL, eclogite facies; GL, glaucophane schist facies; EA, epidote-amphibolite facies; AMP, amphibolite facies; GS, greenschist facies; GRN, granulite facies. (a) Eclogites; (b) garnet amphibolites and (c) country rock gneisses. Experimentally determined reaction curves: (1) Ab = Jd + Qz (Holland, 1983); (2) Pg = Jd + Ky + H_2O (Holland, 1979). Olg-in reaction after Maruyama *et al.* (1983). Plagioclase-out reaction after Ernst & Liu (1998). Wet metapelite solidus and dehydration–melting curve of muscovite (Ms-dm) are according to Le Breton & Thompson (1988). Triple point of Al_2SiO_5 after Holdaway (1971).

boundary for the eclogite facies, and experimentally demonstrated the coexistence of garnet and Ca-amphibole assemblage at ~700 ± 50 °C and 12–16 kbar without producing clinopyroxene.

Eclogites preserved within garnet amphibolites show evidence of the third high-*P* and high-*T* metamorphism (M3). For example, subhedral to euhedral prismatic porphyroblasts of Amp3 occurs in severely amphibolitized eclogites (e.g. sample 03–18; Fig. 3d,e). This amphibole contains inclusions of phengite, epidote, plagioclase ($An_{6–11}$), apatite, rutile and symplectitic aggregates of Cpx3 + Pl2 (Fig. 3d), suggesting that porphyroblastic Amp3 grew during prograde metamorphism after the retrograde stage of the second high-*P* metamorphic event. Amp3 in the matrix show zoning, with Mg-taramite/taramite cores to pargasite/Fe-pargasite rims. These rims are in equilibrium with the rims of plagioclase (An_{16}) in the matrix of the eclogites (Fig. 3e). Plagioclase is also zoned from albite (An_7) cores to oligoclase (An_{21}) rims, suggesting that the *P–T* path of the eclogites crossed the oligoclase-in reaction (Maruyama *et al*., 1983). Ph2 is replaced by a symplectite of biotite and Pl3 ($An_{11–22}$) at its rim. Euhedral pargasite coexists with biotite and Pl3 symplectite (Fig. 3f). Hence, the prograde metamorphism of the third metamorphic event is characterized by the mineral assemblage pargasite/Fe-pargasite, oligoclase and biotite, which is suggestive of amphibolite facies conditions (M3-E2; Fig. 10a).

In the latter part of the metamorphic history, garnet, Ep2 and amphibole (Amp2, Amp3) in the eclogites are partly replaced by chlorite and biotite along their rims and cracks. The replacement of garnet and Amp2 by chlorite, biotite, plagioclase and K-feldspar (e.g. Fig. 4c) in garnet amphibolites suggest retrograde metamorphism of the greenschist facies (M3-E3 & M3-G3; Fig. 10a,b).

Metamorphism of the country rock gneisses

The prograde stage of the epidote-amphibolite facies (M3-P1) is defined by the minerals included within porphyroblastic plagioclase, i.e. Ep1, Ph1 (Si < 6.67 p.f.u.), quartz, K-feldspar, Bt1, Ca-amphibole [Mg-hornblende (TiO_2 = 0.02–0.05 wt%)] (sample KG-432). The mineral assemblage of the inclusions yields metamorphic conditions of 477 °C and 10 kbar for the prograde stage (M3-P1) of the pelitic gneisses, whereas the composition of plagioclase, Ph2, Ep2 and Bt2 in the matrix suggests peak metamorphic conditions (M3-P2) of 635 °C and 13 kbar for the same sample (Fig. 10c).

The mineral assemblage of the peak *P–T* conditions (M3-P2) for samples 03–37 and KG-430 are garnet, Ph2, plagioclase, Bt2, quartz and rutile and the *P–T* conditions estimated by THERMOCALC are 710–745 °C and 14–15 kbar (Table 6; Fig. 10c). Maximum Si contents of Ph2 in the matrix (Si < 6.63 p.f.u.) and Ph1 (Si < 6.88 p.f.u.) included within porphyroblastic plagioclase and zircon in pelitic and granitic gneisses also suggest relatively HP conditions, with minimum pressure of 13 kbar at 700 °C (Massonne & Schreyer, 1987). In summary, the peak metamorphic conditions (M3-P2) for the country rock gneisses are 635–745 °C and 13–15 kbar.

The estimated peak *P–T* conditions (samples 03–37 & KG-430) exceed the temperature of the wet metapelite solidus and lie close to the muscovite dehydration–melting curve (Le Breton & Thompson, 1988), indicating incipient partial melting within the country rock gneisses (Fig. 10c). The *P–T* estimates for sample KG-432 do not reach the wet metapelite solidus, and it shows no evidence of partial melting. Finally, phengite and garnet were replaced by chlorite, biotite, and the country rock gneisses retrograded into the greenschist facies conditions (M3-P3) (Fig. 10c).

Metamorphic evolution and correlation of metamorphism of the eclogites, garnet amphibolites and the country rock gneisses

The estimated *P–T* evolutions of the eclogites, garnet amphibolites and country rocks gneisses in the Aktyuz area are summarized in Fig. 11. The eclogites record three metamorphic events (M1, M2 & M3), whereas the country rock gneisses and the garnet amphibolite occurring at the margins of the eclogites record a single metamorphic event (M3).

A relict MP–HT metamorphism in the Aktyuz eclogites was described by Orozbaev *et al*. (2007). This is the first metamorphic event (M1) of the amphibolite/epidote-amphibolite facies conditions (560–650 °C and 4–10 kbar). Orozbaev *et al*. (2007) also described the prograde stage (M2-E1) of the epidote-blueschist facies conditions (330–570 °C; 8–16 kbar), which documents the beginning of the second HP–LT metamorphism (M2) in the eclogites. In this study, we have constrained the peak metamorphic conditions of the eclogite facies (M2-E2; 550–660 °C and 21–23 kbar) and determined a retrograde stage to epidote-amphibolite facies conditions (M2-E3; 545–565 °C and 10–11 kbar). The metamorphic sequence from the M2-E1 to the peak M2-E2 and subsequent M2-E3 suggest a clockwise *P–T* path for the second HP–LT metamorphic event. The eclogites record evidence of the third HP–HT metamorphic event, i.e. with prograde metamorphism reaching amphibolite facies conditions, labelled as stage M3-E2. The final cooling stage (M3-E3) was greenschist facies retrogression.

The third HP–HT metamorphic event is well documented in the garnet amphibolites and country rock gneisses. The garnet amphibolites show a clockwise *P–T* path, with prograde conditions (M3-G1) of 600–640 °C and 11–12 kbar through the peak metamorphic conditions (M3-G2) with 675–735 °C and 14–15 kbar to greenschist facies conditions (M3-G3). The country rock gneisses also record a clockwise *P–T* path with 475 °C and 10 kbar for the prograde stage (M3-P1) through the peak metamorphic conditions (M3-P2) of

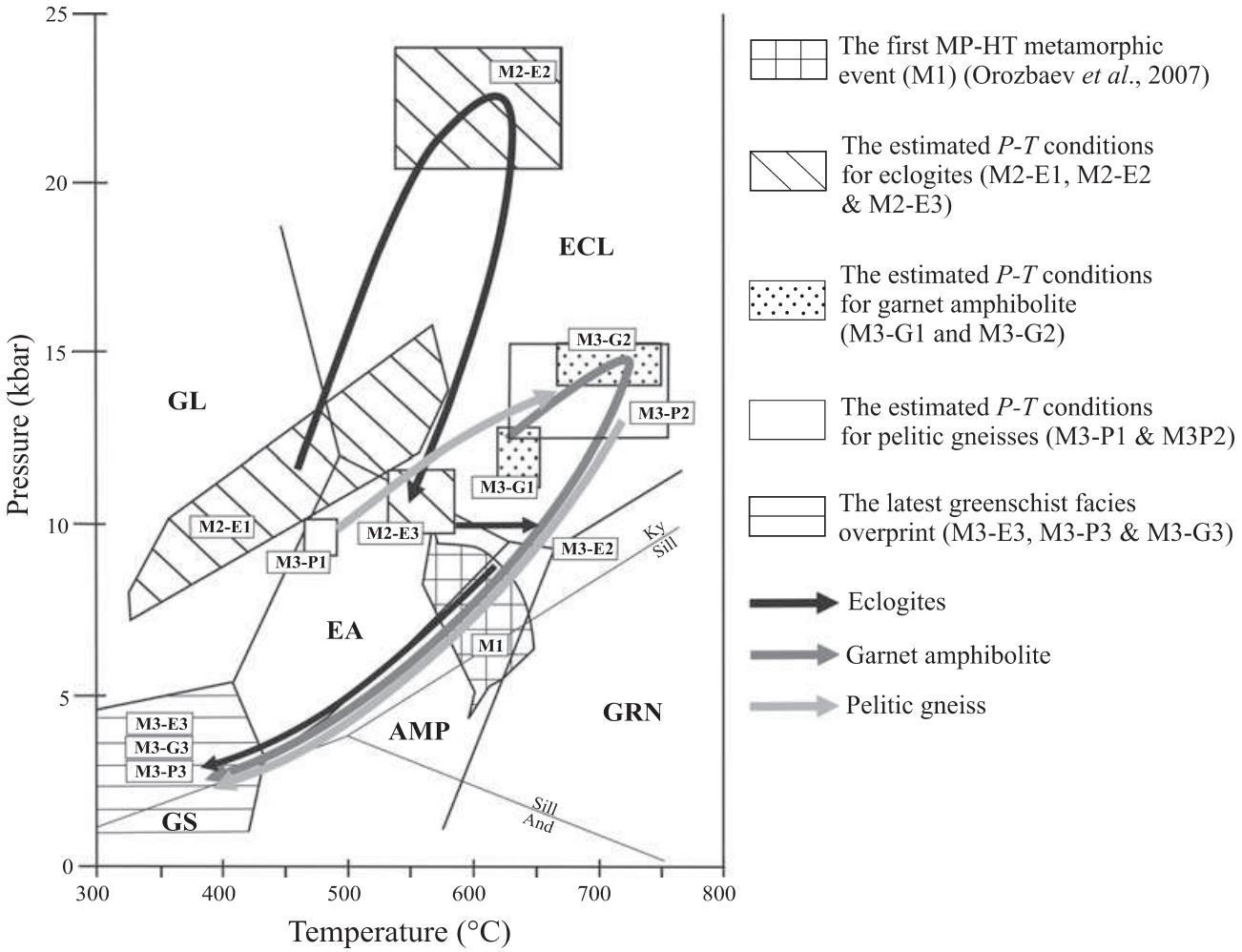

Fig. 11. Summary of *P–T* evolution of the Aktyuz HP metamorphic rocks.

635–745 °C and 13–15 kbar to the greenschist facies stage (M3-P3), which is similar to the *P–T* path obtained for the garnet amphibolites (Fig. 11).

The *P–T* conditions estimated for the prograde, peak and subsequent retrograde stages in the garnet amphibolites and country rock gneisses are identical, which implies that the third metamorphic event deduced from the eclogite-garnet amphibolite bodies is equivalent to the metamorphism of the country rock gneisses. This suggests that the Aktyuz eclogites did not share their *P–T* path of the first and second metamorphic events with the country rock gneisses. The eclogites have been altered into garnet amphibolites that shared their *P–T* path with the surrounding country rock gneisses only during the third metamorphic event.

TECTONIC IMPLICATIONS

The first MP–HT metamorphic event (M1) of the amphibolite/epidote-amphibolite facies conditions in the eclogites is thought to be an early and relatively high-temperature metamorphism before the eclogitic HP–LT metamorphism (Orozbaev *et al.*, 2007). This type of metamorphism before the HP–LT metamorphic event has been described from several metamorphic terranes, including the Franciscan complex (Wakabayashi, 1990), the Iron Mountain-Gee Point area in the North Cascades (Brown *et al.*, 1982) and the Kiziltepe ophiolites in Turkey (Dilek & Whitney, 1997). These studies suggested that the tectonic setting of MP–HT metamorphism of the amphibolite facies before the HP–LT metamorphism of the blueschist to eclogite facies occurred at the metamorphic sole of ophiolites during intra-oceanic subduction or in a subduction zone, with a heat source from hot hangingwall during inception of the subduction. We propose that the MP–HT amphibolite facies metamorphism (M1) in the Aktyuz eclogites formed during the inception of subduction of oceanic lithosphere beneath the continental crust, where the initial thermal condition of that continental crust is sufficiently high

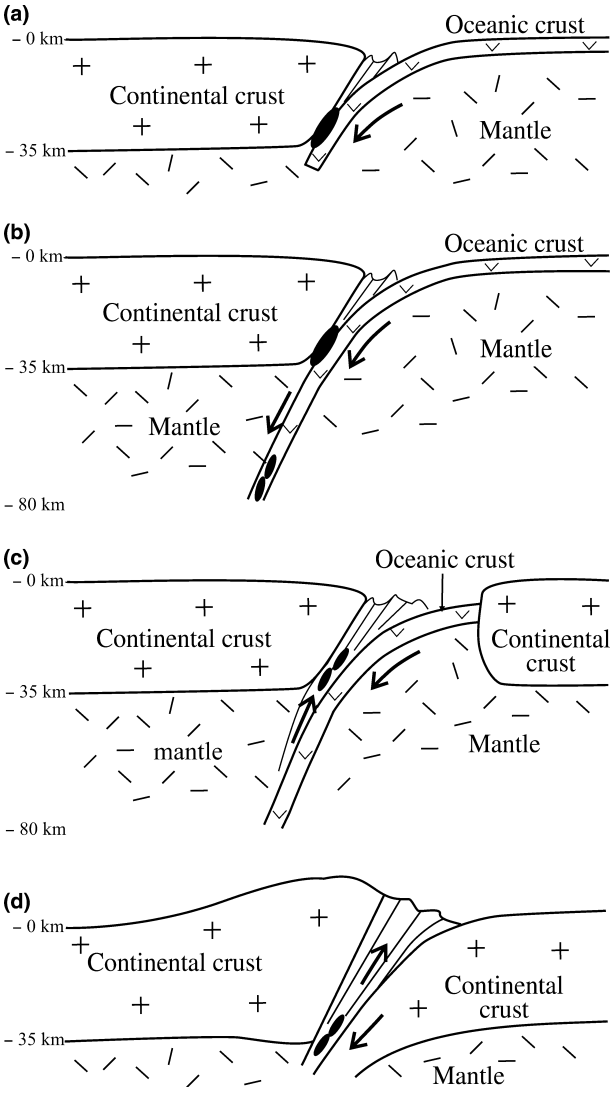

Fig. 12. Schematic geodynamic evolution of the Aktyuz HP metamorphic rocks. (a) The first MP–HT metamorphic event (M1) of the amphibolite/epidote-amphibolite facies conditions in the eclogites occurred during the inception of subduction of oceanic lithosphere beneath the continental crust, with accretion to the hangingwall; (b) sheets or slivers of the amphibolites were stripped off and subsequently dragged to deeper parts of the subduction zone, causing the second HP–LT metamorphic event of blueschist to eclogite facies metamorphism (M2); (c) exhumation of the eclogites to shallow levels of the subduction zone; (d) continent–continent collision setting responsible for the third HP–HT metamorphism (M3) of the Aktyuz country rock gneisses and garnet amphibolites.

to comprise the heat source (Doin & Henry, 2001). At this stage, most of the amphibolites were accreted to the hangingwall (Fig. 12a). Continuous subduction resulted in cooling of the hangingwall (Toksöz *et al.*, 1971; Peacock, 1996), causing the second HP-LT metamorphic event of the blueschist to eclogite facies metamorphism (M2-E1) (Fig. 12b). Some sheets or slivers of the amphibolites were stripped off from hangingwall and were subsequently dragged to deeper parts up to the eclogite facies conditions of the subduction zone (M2-E2; Fig. 12b). This event is documented in subduction zone metamorphism with low geothermal gradient. The Rb–Sr mineral isochron age of 749 ± 14 Ma for the eclogite (Tagiri *et al.*, 1995) is thought to be the timing of the second HP–LT metamorphic event in the Aktyuz eclogites. The eclogites subsequently exhumed to shallow levels in the subduction zone (M2-E3; Fig. 12c).

The *P–T* conditions (635–745 °C; 13–15 kbar; M3-P2) obtained for the third HP–HT metamorphic event (M3) of the Aktyuz country rock gneisses is similar to the *P–T* conditions (700–800 °C; 13–16 kbar) of the metapelites of the Gagnon terrane in the eastern Grenville Province, Canadian Shield (Indares, 1995). The Gagnon terrane is thought to have been deeply buried and formed during an early stage of a crustal shortening/thickening event (Rivers *et al.*, 1993; Indares, 1995). Furthermore, formation of the Aktyuz garnet amphibolites (675–735 °C; 14–15 kbar; M3-G2) at the margins of the eclogites is similar to eclogite formation in the Weinschenk Island of North-East Greenland (650–780 °C; 15–18 kbar) by crustal imbrication and subhorizontal shortening during a Caledonian collision (Elvevold & Gilotti, 2000). Based on the above, we suggest that a similar continent–continent collision setting with a standard geotherm (e.g. Thompson *et al.*, 2001) was responsible for the third HP–HT metamorphism of the Aktyuz country rock gneisses and garnet amphibolites (Fig. 12d). The collisional event took place before the timing of granite intrusion at 416 Ma (SHRIMP zircon age; Konopelko *et al.*, 2006), and the collision probably correlates with the 481 Ma UHP metamorphism in the Makbal area in the Northern Kyrgyz Tien-Shan (Togonbaeva *et al.*, 2009).

The timings of the proposed tectonometamorphic events (M1, M2 & M3) are not constrained. Regionally, Precambrian-Palaeozoic evolution of the CAOB between 1000 and 440 Ma resulted from several accretionary and collisional tectonic events (Şengör *et al.*, 1993; Bakirov & Maksumova, 2001; Dobretsov & Buslov, 2007; Windley *et al.*, 2007). Additional geochronological and geochemical studies are required to link the metamorphic events in the Aktyuz area with global geodynamic processes. Such geochronological and geochemical data, combined with the results of this study, will give a clear picture of the tectonic processes taking place in a model involving palaeo-ocean closure and subsequent continent–continent collision.

ACKNOWLEDGEMENTS

Constructive reviews by D. Whitney and two anonymous referees and editorial handling by D. Whitney are greatly acknowledged. We thank B. Roser for critical review on the early version of the manuscript. We also thank A. A. Bakirov, O. S. Novgorodtsev,

T. Sakurai, Y. Liu, C. Ishida and M. Akaboshi for their help during field survey. The members of the Geoscience Seminar of Shimane University are thanked for their discussion and suggestions. We very much appreciated the efforts of A. Suzuki of Tohoku University in his Raman spectroscopy analysis of inclusions in zircon. This study was partly supported by JSPS Grant-in-Aid for Scientific Research (B) (No 17340149) to A.T., and the Project ISTC (No KR-712) of the Institute of Geology of NAS KR.

REFERENCES

Aoya, M., 2001. *P–T–D* path of eclogite from the Sambagawa Belt deduced from combination of petrological and microstructural analyses. *Journal of Petrology*, **42,** 1225–1248.

Bakirov, A.B., 1978. *Tektonicheskaya pozitsiya metamorphicheskih kompleksov Tyan-Shanya*. Ilim, Frunze, 261 pp.

Bakirov, A.B., 1989. Osobennosti stroeniya i uslovyi formirovaniya eklogitonosnyh metamorphicheskih formatsyi Tyan'-Shanya. In: *Crystallicheskaya kora v prostranstve i vremeni – metamorphicheskie i gidrotermal'nye protsessy* (eds Zharikov, V.A. & Fonarev, V.I.), pp. 193–203. Nauka, Moscow.

Bakirov, A.B. & Korolev, V.G., 1979. Vozrast drevneishih porod Tyan'-Shanya. *Izvestia Academii Nauk SSSR (Seriya Geologicheskaya)*, **7,** 143–146.

Bakirov, A.B. & Maksumova, R.A., 2001. Geodynamic evolution of the Tien-Shan lithosphere. *Russian Geology and Geophysics*, **42,** 1359–1366.

Bakirov, A.B., Dobretsov, N.L., Lavrent'ev, Y.G. & Usova, L.V., 1974. Eklogity Atbashinskogo hrebta, Tyan'-Shan'. *Doklady Academii nauk SSSR*, **215,** 677–680.

Bakirov, A.B., Tagiri, M. & Sakiev, K.S., 1998. Rocks of ultrahigh-pressure metamorphic facies in the Tien Shan. *Russian Geology and Geophysics*, **39,** 1709–1721.

Bakirov, A.B., Tagiri, M., Sakiev, K.S. & Ivleva, E., 2003. The Lower Precambrian rocks in the Tien-Shan and their geodynamic settings. *Geotectonics*, **37,** 368–380.

Bakirov, A.A., Togonbaeva, A.A., Takasu, A. *et al*., 2006. HP and UHP metamorphic rocks in the Makbal area of Northern Tien-Shan, Kyrgyzstan. *Abstracts of the 113th Annual Meeting of the Geological Society of Japan*. Kochi, Japan, 139.

Baldwin, J.A., Powell, R., Williams, M.L. & Goncalves, P., 2007. Formation of eclogite, and reaction during exhumation to mid-crustal levels, Snowbird tectonic zone, western Canadian Shield. *Journal of Metamorphic Geology*, **25,** 953–974.

Bence, A.E. & Albee, A.L., 1968. Empirical correction factors for the electron microanalysis of silicates and oxides. *Journal of Geology*, **76,** 382–403.

Brown, E.H., Wilson, D.L., Armstrong, R.L. & Harakal, J.E., 1982. Petrologic, structural, and age relations of serpentinite, amphibolite, and blueschist in the Shuksan Suite of the Iron Mountain-Gee Point area, North Cascades, Washington. *Geological Society of America Bulletin*, **93,** 1087–1098.

Burtman, V.S., Skobelev, S.F. & Molnar, P., 1996. Late Cenozoic slip on the Talas-Ferghana fault, the Tien-Shan, central Asia. *Geological Society of America Bulletin*, **108,** 107–118.

Chopin, C., 1984. Coesite and pure pyrope in high-grade blueschists of the western Alps: a first record and some consequences. *Contributions to Mineralogy and Petrology*, **86,** 107–118.

Compagnoni, R., Hirajima, T. & Chopin, C., 1995. Ultrahigh-pressure metamorphic rocks in the Western Alps. In: *Ultrahigh-Pressure Metamorphism* (eds Coleman, R.G. & Wang, X.), pp. 206–243. Cambridge University Press, Cambridge.

Dale, J. & Holland, T.J.B., 2003. Geothermobarometry, *P–T* paths and metamorphic field gradients of high-pressure rocks from the Adula Nappe, Central Alps. *Journal of Metamorphic Geology*, **21,** 813–829.

Dilek, Y. & Whitney, D.L., 1997. Counterclockwise *P–T–t* trajectory from the metamorphic sole of a Neo-Tethyan ophiolite (Turkey). *Tectonophysics*, **280,** 295–310.

Djenchuraeva, R.D., Borisov, F.I., Pak, N.T. & Malyukova, N.N., 2008. Metallogeny and geodynamics of the Aktiuz-Boordu Mining District, Northern Tien Shan, Kyrgyzstan. *Journal of Asian Earth Sciences*, **32,** 280–299.

Dobretsov, N.L. & Buslov, M.M., 2007. Late Cambrian-Ordovician tectonics and geodynamics of Central Asia. *Russian Geology and Geophysics*, **48,** 71–82.

Dobretsov, N.L., Sobolev, N.V., Shatsky, V.S., Coleman, R.G. & Ernst, W.G., 1995. Geotectonic evolution of diamondiferous paragneisses, Kokchetav complex, northern Kazakhstan – the geologic enigma of ultra-high pressure crustal rocks within a Palaeozoic foldbelt. *Island Arc*, **4,** 267–279.

Doin, M.-P. & Henry, P., 2001. Subduction initiation and continental crust recycling: the roles of rheology and eclogitization. *Tectonophysics*, **342,** 163–191.

Ellis, E. & Green, D., 1979. An experimental study of the effect of Ca upon garnet-clinopyroxene Fe–Mg exchange equilibria. *Contributions to Mineralogy and Petrology*, **71,** 13–22.

Elvevold, S. & Gilotti, J.A., 2000. Pressure-temperature evolution of retrogressed kyanite eclogites, Weinschenk Island, North-East Greenland Caledonides. *Lithos*, **53,** 127–147.

Enami, M. & Nagasaki, A., 1999. Prograde *P–T* path of kyanite eclogites from Junan in the Sulu ultrahigh-pressure province, eastern China. *Island Arc*, **8,** 459–474.

Engvik, A.K. & Andersen, T.B., 2000. Evolution of Caledonian deformation fabrics under eclogite and amphibolite facies at Vardalsneset, Western Gneiss Region, Norway. *Journal of Metamorphic Geology*, **18,** 241–257.

Ernst, W.G., 1971. Do mineral parageneses reflect unusually high pressure conditions of Franciscan metamorphism? *American Journal of Science*, **271,** 81–108.

Ernst, W.G. & Liu, J., 1998. Experimental phase-equilibrium study of Al- and Ti-contents of calcic amphibole in MORB – A semiquantitative thermobarometer. *American Mineralogist*, **83,** 952–969.

Gao, J. & Klemd, R., 2003. Formation of HP-LT rocks and their tectonic implications in the western Tianshan Orogen, NW China: geochemical and age constraints. *Lithos*, **66,** 1–22.

Gao, J., Klemd, R., Zhang, L., Wang, Z. & Xiao, X., 1999. *P–T* path of high pressure – low temperature rocks and tectonic implications in the western Tianshan Mountains (NW China). *Journal of Metamorphic Geology*, **17,** 621–636.

Graham, C.M. & Powell, R., 1984. A garnet-hornblende geothermometer: calibration, testing, and application to the Pelona Schist, Southern California. *Journal of Metamorphic Geology*, **2,** 13–31.

Holdaway, M.J., 1971. Stability of andalusite and the aluminium silicate phase diagram. *American Journal of Science*, **271,** 97–131.

Holland, T.J.B., 1979. Experimental determination of the reaction Paragonite = Jadeite + Kyanite + H_2O, and internally consistent thermodynamic data for part of the system Na_2O–Al_2O_3–SiO_2–H_2O with applications to eclogite and blueschists. *Contributions to Mineralogy and Petrology*, **68,** 293–301.

Holland, T.J.B., 1983. Experimental determination of the activities in disordered and short-range ordered jadeitic pyroxenes. *Contributions to Mineralogy and Petrology*, **82,** 214–220.

Holland, T.J.B. & Blundy, J.D., 1994. Non-ideal interactions in calcic amphiboles and their bearing on amphibole-plagioclase thermometry. *Contributions to Mineralogy and Petrology*, **116,** 433–447.

Holland, T.J.B. & Powell, R., 1998. An internally consistent thermodynamic data set for phases of petrological interest. *Journal of Metamorphic Geology*, **16,** 309–343.

Indares, A., 1995. Metamorphic interpretation of high-pressure–temperature metapelites with preserved growth zoning in garnet, eastern Grenville Province, Canadian Shield. *Journal of Metamorphic Geology*, **13,** 475–486.

Ishida, C., Takasu, A., Sakurai, T., Akaboshi, M. & Tagiri, M., 2004. Coesite bearing Grt-Cld-Tlc schist from Makbal, Kyrgyzstan. *Abstracts of the 111th Annual Meeting of the Geological Society of Japan*. Chiba, Japan, 274.

Katayama, I., Parkinson, C.D., Okamoto, K., Nakajima, Y. & Maruyama, S., 2000. Supersilicic clinopyroxene and silica exsolution in UHPM eclogite and pelitic gneiss from the Kokchetav massif, Kazakhstan. *American Mineralogist*, **85,** 1368–1374.

Kiselev, V.V., 1999. U–Pb (po zirconam) geochronologiya magmaticheskih proyavlenyi Severnogo Tyan'-Shanya. *Kyrgyz Respublikasynyn Uluttuk Ilimder Akademiyasynyn Kabarlary*, Special issue ''Problemy geologii i geografii v Kyrgyzstane'', 21–33.

Kiselev, V.V., Apoyarov, F.H., Komarevtsev, V.T. & Tsyganok, E.N., 1993. Izotopnyi vozrast zirkonov kristallicheskih kompleksov Tyan'-Shanya. In: *Rannyi dokembryi Zentral' noaziatskogo skladchatogo poyasa* (ed. Kozakov, I.K.), pp. 99–115. Nauka, Moscow.

Klemd, R., Schröter, F., Will, T.M. & Gao, J., 2002. *PT*-evolution of glaucophane-clinozoisite bearing HP–LT rocks in the western Tianshan orogeny, NW China. *Journal of Metamorphic Geology*, **20,** 239–254.

Konopelko, D.L., Seltmann, R., Biske, G.S., Matukov, D.I. & Sergeev, S.A., 2006. Hercynian magmatism in the Tien Shan: new SHRIMP ages and metallogenic implications. In: *Porphyry and Epithermal Deposits of the Chatkal-Kurama Region: Abstracts and Programme* (eds Seltmann, R., Cook, N., Koneev, R. & Dolgopolova, A.), pp. 31–35. Field Workshop in Uzbekistan, Tashkent.

Kurz, W. & Froitzheim, N., 2002. The exhumation of eclogite-facies metamorphic rocks – a review of models confronted with examples from the Alps. *International Geology Review*, **44,** 702–743.

Le Breton, N. & Thompson, A.B., 1988. Fluid-absent (dehydration) melting of biotite in metapelites in the early stages of crustal anatexis. *Contributions to Mineralogy and Petrology*, **99,** 226–237.

Leake, B.E., Wooley, A.R., Arps, C.E.S. *et al*., 1997. Nomenclature of amphiboles; report of the Subcommittee on Amphiboles of the International Mineralogical Association Commission on New Minerals and Mineral Names. *Mineralogical Magazine*, **61,** 295–321.

Lin, W. & Enami, M., 2006. Prograde pressure-temperature path of jadeite-bearing eclogites and associated high-pressure/low-temperature rocks from western Tianshan, northwest China. *Island Arc*, **15,** 483–502.

Liu, F.L., Gerdes, A. & Xue, H.M., 2009. Differential subduction and exhumation of crustal slices in the Sulu HP–UHP metamorphic terrane: insights from mineral inclusions, trace elements, U-Pb and Lu-Hf isotope analyses of zircon in orthogneisses. *Journal of Metamorphic Geology*, **27,** 805–825.

Lü, Z., Zhang, L., Du, J. & Bucher, K., 2009. Petrology of coesite-bearing eclogite from Habutengsu Valley, western Tianshan, NW China and its tectonometamorphic implication. *Journal of Metamorphic Geology*, **27,** 773–787.

Maruyama, S., Suzuki, K. & Liou, J.G., 1983. Grenschist-amphibolite transition equilibria at low pressures. *Journal of Petrology*, **24,** 605–634.

Massonne, H.-J. & Schreyer, W., 1987. Phengite geobarometry based on the limiting assemblage with K-feldspar, phlogopite and quartz. *Contributions to Mineralogy and Petrology*, **96,** 212–224.

Medaris, L.G., Fournelle, J.H., Ghent, E.D., Jelinek, E. & Misar, Z., 1998. Prograde eclogite in the Gföhl Nappe, Czech Republic: new evidence on Variscan high-pressure metamorphism. *Journal of Metamorphic Geology*, **16,** 563–576.

Miyagi, Y. & Takasu, A., 2005. Prograde eclogites from the Tonaru epidote amphibolite mass in the Sambagawa Metamorphic Belt, central Shikoku, southwest Japan. *Island Arc*, **14,** 215–235.

Moore, D.E., 1984. Metamorphic history of a high-grade blueschist exotic block from the Franciscan Complex, California. *Journal of Petrology*, **25,** 136–150.

Morimoto, N., 1988. Nomenclature of pyroxenes. *American Mineralogist*, **73,** 1123–1133.

Nikolaev, V.A., 1933. On the most important structural line of the Tien-Shan. *Zapiski Vserossiyskogo Mineralogicheskogo Obshestva*, **2,** 347–354.

Okay, A.I., 1989. An exotic eclogite blueschist slice in a Barrovian-style metamorphic terrain, Alanya nappes, Southern Turkey. *Journal of Petrology*, **30,** 107–132.

Orozbaev, R.T., Takasu, A., Tagiri, M., Bakirov, A.B. & Sakiev, K.S., 2007. Polymetamorphism of Aktyuz eclogites (northern Kyrgyz Tien-Shan) deduced from inclusions in garnets. *Journal of Mineralogical and Petrological Sciences*, **102,** 150–156.

Peacock, S.M., 1996. Thermal and petrologic structure of subduction zones. In: *Subduction: Top to Bottom* (ed. Bebout, G.E.), Geophysical Monograph, Series 96, pp. 119–133. AGU, Washington DC.

Powell, R., 1985. Regression diagnostic and robust regression in geothermometer/geobarometer calibration: the garnet-clinopyroxene geothermometer revisited. *Journal of Metamorphic Geology*, **3,** 231–243.

Powell, R. & Holland, T.J.B., 1994. Optimal geothermometry and geobarometry. *American Mineralogist*, **79,** 120–133.

Ravna, E.J.K., 2000. The garnet-clinopyroxene Fe^{2+}-Mg geothermometer: an updated calibration. *Journal of Metamorphic Geology*, **18,** 211–219.

Ravna, E.J.K. & Terry, M.P., 2004. Geothermobarometry of UHP and HP eclogites and schists – an evaluation of equilibria among garnet-clinopyroxene-kyanite-phengite-quartz/coesite. *Journal of Metamorphic Geology*, **22,** 579–592.

Rivers, T., van Gool, J. & Connelly, J., 1993. Contrasting styles of crustal shortening in the northern Grenville orogen. *Geology*, **21,** 1127–1130.

Schumacher, J.C., 1991. Empirical ferric iron corrections: necessity, assumptions, and effects on selected geothermobarometers. *Mineralogical Magazine*, **55,** 3–18.

Şengör, A.M.C., Natal'in, B.A. & Burtman, V.S., 1993. Evolution of the Altaid tectonic collage and Paleozoic crustal growth in Eurasia. *Nature*, **364,** 299–307.

Smith, D.C., 1988. A review of the peculiar mineralogy of the ''Norwegian Coesite Eclogite Province'', with crystal-chemical, petrological, geochemical and geodynamical notes and an extensive bibliography. In: *Eclogites and Eclogite-Facies Rocks* (ed. Smith, D.C.), pp. 1–206. Elsevier, Amsterdam.

Sobolev, N.V., Dobretsov, N.L.Bakirov, A.B. & Shatsky, V.S., 1986. Eclogites from various types of metamorphic complexes in the USSR and the problems of their origin. In: *Blueschist and Eclogites* (eds, Evans, B.W. & Brown, E.H.), *Geological Society of America Memoir*, **164,** 349–363.

Song, S.G., Yang, J.S., Xu, Z.Q., Liou, J.G. & Shi, R.D., 2003. Metamorphic evolution of the coesite-bearing ultrahigh-pressure terrane in the North Qaidam, Northern Tibet, NW China. *Journal of Metamorphic Geology*, **21,** 631–644.

Štípská, P., Pitra, P. & Powell, R., 2006. Separate or shared metamorphic histories of eclogites and surrounding rocks? An example from the Bohemian Massif. *Journal of Metamorphic Geology*, **24,** 219–240.

Tagiri, M. & Bakirov, A.B., 1990. Quartz pseudomorph after coesite in garnet from a garnet-chloritoid-talc schist, northern Tien-Shan, Kirghis SSR. *Proceedings of Japan Academy*, **66,** Ser. B, 135–139.

Tagiri, M., Yano, T., Bakirov, A.B., Nakajima, T. & Uchiumi, S., 1995. Mineral parageneses and metamorphic *P–T* path of ultrahigh-pressure eclogites from Kyrgyzstan, Tien-Shan. *Island Arc*, **4,** 280–292.

Tagiri, M., Takasu, A., Bakirov, A.B. & Sakiev, K.S., 2006. Coesite schist and metamorphic xenoblock, Makbal, Kyrgyz Tien Shan. *Abstracts of the 113th Annual Meeting of the Geological Society of Japan*. Kochi, Japan, 246.

Takasu, A., 1984. Prograde and retrograde eclogites in the Sambagawa metamorphic belt, Besshi District, Japan. *Journal of Petrology*, **25,** 619–643.

Takasu, A., 1989. *P–T* histories of peridotite and amphibolite tectonic blocks in the Sambagawa metamorphic belt, Japan. In: *Evolution of Metamorphic Belts* (eds, Daly, J.S., Cliff, R.A. & Yardley, B.W.D.), *Geological Society by Blackwell Scientific Publications, Special Publication*, **43,** 533–538.

Thompson, A.B., Schulmann, K., Jezek, J. & Tolar, V., 2001. Thermally softened continental extensional zones (arcs and rifts) as precursors to thickened orogenic belts. *Tectonophysics*, **332,** 115–141.

Togonbaeva, A.A., Takasu, A., Bakirov, A.A. *et al*., 2009. CHIME monazite ages of garnet-chloritoid-talc schists in the Makbal Complex, Northern Kyrgyz Tien-Shan: first report of the age of the UHP metamorphism. *Journal of Mineralogical and Petrological Sciences*, **104,** 77–81.

Toksöz, M.N., Minear, J.W. & Julian, B.R., 1971. Temperature field and geophysical effects of a downgoing slab. *Journal of Geophysical Research*, **76,** 1113–1138.

Tracy, R.J., 1982. Compositional zoning and inclusions in metamorphic minerals. In: *Characterization of Metamorphism Through Mineral Equilibria* (ed. Ferry, J.M.), Mineralogical Society of America, Washington, DC. *Reviews in Mineralogy*, **10,** 355–397.

Volkova, N.I. & Budanov, V.I., 1999. Geochemical discrimination of metabasalt rocks of the Fan-Karategin transitional blueschist/greenschist belt, South Tien Shan, Tajikistan: seamount volcanism and accretionary tectonics. *Lithos*, **47,** 201–216.

Wakabayashi, J., 1990. Counterclockwise *P–T–t* path from amphibolites, Franciscan complex, California: relics from the early stages of subduction zone metamorphism. *Journal of Geology*, **98,** 657–680.

Wang, X.M., Liou, J.G. & Mao, H.G., 1989. Coesite-bearing eclogites from the Dabie mountains in central China. *Geology*, **17,** 1085–1088.

Wei, C.J., Powell, R. & Zhang, L.F., 2003. Eclogites from the south Tianshan, NW China: petrological characteristic and calculated mineral equilibria in the Na_2O–CaO–FeO–MgO–Al_2O_3–Si_2O–H_2O system. *Journal of Metamorphic Geology*, **21,** 163–179.

Whitney, D.L. & Evans, B.W., 2010. Abbreviations for names of rock-forming minerals. *American Mineralogist*, **95,** 185–187.

Windley, B.F., Alexeiev, D., Xiao, W., Kröner, A. & Badarch, G., 2007. Tectonic models for accretion of the Central Asian Orogenic Belt. *Journal of the Geological Society, London*, **164,** 31–47.

Yang, J., Liu, F., Wu, C. *et al*., 2005. Two ultrahigh-pressure metamorphic events recognized in the central orogenic belt of China: evidence from the U-Pb dating of coesite-bearing zircons. *International Geology Review*, **47,** 327–343.

Zhang, L., Song, S., Liou, J.G., Ai, Y. & Li, X., 2005. Relict coesite exsolution in omphacite from western Tianshan eclogites, China. *American Mineralogist*, **90,** 181–186.

Zhang, L., Ai, Y., Li, X. *et al*., 2007. Triassic collision of western Tianshan orogenic belt, China: evidence from SHRIMP U-Pb dating of zircon from HP-UHP eclogitic rocks. *Lithos*, **96,** 266–280.

Received 23 May 2009; revision accepted 12 January 2010.